isvr Institute of Sound and Vibration Research

An Introduction to FE-PST the combined use of Finite Element Analysis and Periodic Structure Theory

D.J. Mead

ISVR Technical Memorandum No 959

March 2006

University of Southampton

SCIENTIFIC PUBLICATIONS BY THE ISVR

Technical Reports are published to promote timely dissemination of research results by ISVR personnel. This medium permits more detailed presentation than is usually acceptable for scientific journals. Responsibility for both the content and any opinions expressed rests entirely with the author(s).

Technical Memoranda are produced to enable the early or preliminary release of information by ISVR personnel where such release is deemed to the appropriate. Information contained in these memoranda may be incomplete, or form part of a continuing programme; this should be borne in mind when using or quoting from these documents.

Contract Reports are produced to record the results of scientific work carried out for sponsors, under contract. The ISVR treats these reports as confidential to sponsors and does not make them available for general circulation. Individual sponsors may, however, authorize subsequent release of the material.

UNIVERSITY OF SOUTHAMPTON

INSTITUTE OF SOUND AND VIBRATION RESEARCH

DYNAMICS GROUP

An Introduction to FE-PST – the combined use of Finite Element Analysis and Periodic Structure Theory

by

D.J. Mead

ISVR Technical Memorandum No: 959

March 2006

Authorised for issue by
Professor M.J. Brennan
Group Chairman

ABSTRACT

Periodic structure theory is concerned with the analysis of arrays of identical structural elements joined together end to end and/or side by side. This paper shows how it can be combined with the finite element method to study both free and forced harmonic wave propagation in uniform rails, bars and structural stiffeners. It first reviews the fundamentals of mono-coupled periodic structure theory by using it with a simple finite element to analyse longitudinal wave motion in a uniform bar. Free and forced harmonic motion of both infinite and finite bars are considered.

At high frequencies the cross-sectional distortion of the bar is allowed for by sub-dividing a narrow slice of the bar into finite elements. Each slice then becomes a periodic element in a multi-coupled structure to which the author's multi-coupled theory of free wave propagation can be applied. This theory is reviewed and formally extended to deal with forced vibrations of both infinite and finite multi-coupled systems. Applying it, one can use just a single narrow slice to predict accurate wave numbers or decay factors of propagating or evanescent waves in bars of any uniform cross section and length. The size of the matrices involved in the calculations depends only on the number of coordinates defining the cross-sectional displacements of the single slice and not on the number of slices in the system length. For this reason, the slices may be extremely narrow. Numerical problems permitting, the narrower they are the more accurate the results.

Computed results are presented for the wave numbers and decay factors of free in-plane wave motion in a thin uniform flat plate of finite width. Up to six simple finite elements were employed in the single slice. The response of this plate to in-plane harmonic forces is also examined and the influence of evanescent wave motion is briefly considered. Comparisons are made with results from simple engineering theories (the Euler-Bernoulli and Timoshenko beam theories) and from the exact theory of elasticity.

1. INTRODUCTION

Periodic structure theory (PST) in conjunction with finite element analysis (FE) has now been used for a nu ber of years to study harmonic wave propagation along uniform bars, rails and open-section structural members. As these structures are usually very long and the wavelengths of their high frequency vibrations are very short, the usual type of FE calculation for their free or forced vibrations requires very many elements for accurate response levels to be computed . This, in turn, can lead to enormous global stiffness and mass matrices and very long computation times. The size of these is greatly reduced when periodic structure theory is invoked.

The history of this process can be traced back to 1973 when the present author published his general theory of wave propagation in periodic structures [1]. As implied by this phrase, the theory is concerned with *wave* motion, rather than with the *normal modes* of vibration for which FE methods are frequently and very conveniently used. The first step in the PST approach is to find the 'propagation constants' of the wave motion across a single 'periodic element' of the system. The periodic element is the fundamental structural unit which is repeated periodically and identically throughout the whole structure. A propagation constant is the phase difference or exponential decay factor across the element when certain time-harmonic 'characteristic waves' are progressing. If there are N_L periodic elements in a unit length of the structure, the wave number of the motion is N_L times the propagation constant.

An FE method to find wave numbers of waves in long uniform bars of arbitrary cross section was first used in 1973 by Aalami [2], but this did not involve PST. In essence, he found the frequency of a bar vibrating harmonically in a sinusoidal mode of prescribed wave number. A single half-wavelength of the bar was subdivided over its cross section into a finite number of solid elements. Across each of these the displacements varied linearly. The stiffness and mass matrices developed for these were functions of the given wave number (and hence of frequency) so the basic elements in this case would now be classified as spectral finite elements (SFE).

Aalami proceeded to set up the stiffness and mass matrices for the whole system. The cross-sectional deflection and distortion was defined by N_C displacement co-ordinates, so the order of these matrices is N_C x N_C and the corresponding equations of harmonic motion led to an

eigenvalue equation of order N_C x N_C. This yielded N_C frequencies at which waves with the given wavelength could propagate. Dispersion curves were generated for several different structural sections and showed (not unexpectedly) that an increase in the number of elements over the cross section leads to increasing accuracy in the computed frequencies.

Note that Aalami's method only finds the frequencies corresponding to prescribed wavelengths. It does not find wavelengths or wave numbers for given frequencies, as can be done with the PST formulation. Moreover, it cannot find the real frequencies of evanescent waves which have complex wave numbers, simply because these wave numbers cannot be specified in advance. Nor can it accurately predict the frequencies of the better known evanescent waves which decay in space without spatial oscillation.

Now these evanescent wave-types had long been known to exist in periodic structures, their wave numbers having been computed for many different types of structure by periodic structure analysis. However, an element of unrealism hangs over such studies since real engineering periodic structures never exist in practice. On the other hand an FE model of a uniform bar or rail can represent a truly periodic structure if the bar is divided into equal slices (of length δL, say), each of which is subdivided identically into solid finite elements. Since all slices are identical and are coupled identically to their neighbours, each slice clearly constitutes a structural periodic element. Wave motion along this system can be studied by invoking Floquet's theorem for periodic structures (see Brillouin [3]) which relates the N_C displacement co-ordinates $\{q_L\}$ on the left-hand face of the slice to those on the right-hand face, $\{q_R\}$. The theorem simply states that when a free wave passes through a periodic structure $\{q_L\} = \{q_R\}e^{\lambda}$. λ is the propagation constant of the motion and is the unknown found by PST. When it is purely imaginary (= $i\varepsilon$, say) it represents the phase difference between the motions at the two ends of the slice. With N_L elements in a unit length of the structure ($N_L = 1/\delta L$) the total phase difference between the motion at each end of the unit length is $N_L\varepsilon$ and this, of course, is the wave number k of the wave motion. $\{q_L\}$ and $k = N_L\varepsilon$ completely define the deflections and distortions of the whole periodic element (the slice). Global stiffness and mass matrices can be set up and used in an eigenvalue calculation to determine k for a given frequency. This is the essence of PST which can be usefully combined with FE analysis to solve directly for all possible

wave numbers for a given frequency. It extends Aalami's method to include evanescent, non-propagating waves in addition to the sinusoidal propagating waves.

Different methods have been used over the years to set up the relevant dynamic equations for different types of periodic element. They include closed-form receptance solutions for beam-type elements (e.g. rails on sleepers) [5], FE analyses of stiffened plate and shell configurations [6,7, 8] and a simple Rayleigh-Ritz method for a beam element [9] . In all of these studies, the *periodic length* was dictated by the given structural design, e.g. the sleeper-spacing beneath the rail or the spacing of the stiffeners on a plate. But when the rail, bar or stiffener can be considered to be unimpeded by supports and the PST approach is used, the periodic length may be made as small as one wishes, within limits. PST only 'operates' on a single element and the number of FE slices in a unit length of the member does not influence the overall computation time. In principle at least, the slice could be infinitesimally small, so it follows that the length wise variation of its displacement can take the simplest possible linear form. Up to a point, reducing the length of the element enhances the accuracy of the PST-FE calculation which is limited only by the number of elements within a single slice. Too much reduction, however, can lead to computational problems associated with rounding errors etc. and causes the accuracy to deteriorate.

Thompson [10] (following a suggestion from the author) used the combined PST-FE approach to investigate high frequency wave propagation along a railway rail. Although these rails are periodically supported on identical chairs and sleepers (and in consequence have often been quoted as examples of periodic structures) high frequency, noise-producing short waves can pass almost unimpeded over the supports if they are undamped. In that case they can be ignored and long-range vibration transmission along the complicated rail section can be analysed by the combined PST-FE method. All that has to be studied is a single thin slice of rail whose displacements along its short length can vary in the simplest linear form and not in the form of a wave with a specified wave number.

Since Thompson's work, other investigators have modified and extended Aalami's approach to study wave motion along bars and rails, thin-walled cylinders and open-section beams. SFE's of a distinctive form were used in which all displacements varied in the

propagation direction in proportion to e^{ikx} while across the section of each element they varied in simple linear or polynomial forms. The resultant stiffness matrices consisted of sums of up to four matrices, each multiplied by a power of k. Gavric [11] considered thin-walled cylinders and open-section beams with linear or bi-linear variations of displacement across the elements. Widehammer [12] and Finnveden [13] considered uniform bars, describing the cross-sectional displacements in terms of continuous polynomial functions. Nilsson [14] used the same general approach to study structural and acousto-structural configurations which included car tyre sections, conical shells and periodically stiffened plate/shell structures. This method allows wave numbers to be found for given frequencies and *vice versa*, but although it allows complex wave numbers and decay factors of evanescent wave motions to be computed, the only results presented were for undecaying propagating waves.

It is important to observe that in each of references [11] to [14] new stiffness and mass matrices had to be derived for the elements for each type of structure. The elements were developed particularly for studies of unidirectional wave-motion (all displacements being proportional to e^{ikx}) so Nilsson called the technique the *'wave-guide finite element method'* (WFEM') although the elements themselves were special forms of SFE's. More recently Mace *et al* [15] claimed the term 'wave-guide finite element' (WFE) for the PST method of using simple finite elements in studies of unidirectional wave propagation. The elements themselves and their matrices are essentially independent of wave number and can actually be used to study any type of wave or modal motion, not just the unidirectional motion along a wave-guide. As already stated, this approach has the advantage that the element matrices can be obtained from commercial software packages. The WFE's of [11-14] may have better claim to the term but are disadvantaged by requiring new matrices to be formulated for each new problem investigated. Mace *et al* used element matrices from the ANSYS package in conjunction with PST equations first presented in [1] and proceeded to study wave motion in uniform beams, simply-supported plate strips and visco-elastic laminates.

When there are N_C coupling co-ordinates between the adjacent periodic elements, the FE-PST form of WFE analysis yields a quadratic eigenvalue problem for the k's. This is easily reduced [4] to a linear eigenvalue problem of order $2N_C$ x $2N_C$ which is twice that of Aalami's equations but only one half of some of Nilsson's. The $2N_C$ wave numbers found consist of N_C

positive/negative pairs, each pair corresponding to the same wave travelling in either the positive or negative direction. Further manipulation of the equations (see Thompson [10]) can reduce them to the order N_C x N_C from which only one of each eigenvalue pair is computed. The calculation of wave numbers also yields the wave eigenvectors (the $\{q\}$'s) which effectively define the modes of cross-sectional displacement corresponding to each wave.

A point harmonic force at a given location generates waves which travel outwards in both directions from the source and knowing their eigenvectors, one can determine the forced wave amplitudes. If the structure is infinite and uninterrupted, outgoing waves only are generated and combine to produce the total motion. In a finite structure, they are reflected back to the source by the boundaries or other discontinuities and the whole set of outgoing and reflected waves combine in the correct proportions to satisfy the overall boundary conditions of the structure. Viewed in this way, the calculation of the total response now involves a wave motion study, rather than one of forced normal modes. It can yield the response at any point in a bar or rail forced harmonically at any other point.

The purpose of this paper is to show how this can be accomplished and can be regarded as a sequel to the author's general theory of 1973 [1]. It lays a complete foundation for combining PST with FE analysis and extends the former free-wave theory to deal with motion which is forced harmonically at an arbitrary single point. First presented is the most elementary example of a simple uniform bar undergoing longitudinal plane-wave motion. The theory is then developed to deal with wave motion which may include combined longitudinal, flexural, torsional deflections and non-planar cross-sectional deformation. It is then applied to study a thin, uniform flat plate of finite width. Wave numbers (real, imaginary and complex) and harmonic in-plane responses are calculated over very wide frequency ranges and calculated values are compared with those obtained from both simple engineering theories (the Euler-Bernoulli and Timoshenko beam theories) and the exact elasticity theory. The results further expose the high frequency limitations of the Timoshenko beam theory. The significance (or otherwise) of evanescent wave motions is investigated for some special cases of forced vibration.

2. THE PRINCIPLE APPLIED TO FREE LONGITUDINAL WAVE MOTION IN A UNIFORM BAR

2.1 THE DETERMINATION OF THE WAVE NUMBERS

The simplest possible application is to the elastic uniform bar of cross-sectional area A, density ρ and elastic modulus E. Its simplest finite element is of small length δL across which the displacements and direct strains are uniform. A unit length of the bar contains $1/\delta L = N_E$ of these. The longitudinal displacements and axial forces at the left and right hand ends of the element are u_L, u_R, F_L, F_R respectively as in the following Figure 1.

Assume that the direct longitudinal strain in each element between the ends is uniform and the mass of the element is assigned in equal amounts ($\rho A \delta L/2$) to the ends of the element. The stiffness and mass matrices for this element are found to be

$$K = EA/\delta L \begin{bmatrix} 1 & -1 \\ -1 & 1 \end{bmatrix} \quad \text{and} \quad M = \rho A \delta L/2 \begin{bmatrix} 1 & 0 \\ 0 & 1 \end{bmatrix} \tag{1}$$

When the bar undergoes free harmonic wave motion, the element forces and displacements are related through

$$\begin{Bmatrix} F_L \\ F_R \end{Bmatrix} = [K - \omega^2 M] \begin{Bmatrix} u_L \\ u_R \end{Bmatrix} = EA/\delta L \left[\begin{bmatrix} 1 & -1 \\ -1 & 1 \end{bmatrix} - \omega^2 \rho \delta L^2/2E \begin{bmatrix} 1 & 0 \\ 0 & 1 \end{bmatrix} \right] \begin{Bmatrix} u_L \\ u_R \end{Bmatrix} \tag{2}$$

Now $\rho/E = 1/c_L^2$, where c_L is the speed of free longitudinal wave motion in the simple bar. The corresponding wave number is $k_L = \omega/c_L$, so $\omega^2 \rho \delta L^2/2E = k_L^2 \delta L^2/2$.

When a free wave travels through a periodic system of such elements, the displacement and force at the left hand end of any element B are e^{μ} times those at the left hand end of the preceding element A, so

$$\left\{ \begin{array}{c} u_L \\ F_L \end{array} \right\}_B = e^{\mu} \left\{ \begin{array}{c} u_L \\ F_L \end{array} \right\}_A \tag{3}$$

For compatibility and equilibrium between the elements A and B:

$$\left\{ \begin{array}{c} u_L \\ F_L \end{array} \right\}_B = \left\{ \begin{array}{c} u_R \\ -F_R \end{array} \right\}_A \qquad \text{so} \qquad \left\{ \begin{array}{c} u_L \\ F_L \end{array} \right\}_A = e^{\mu} \left\{ \begin{array}{c} u_R \\ -F_R \end{array} \right\}_A \tag{4}$$

Substituting these into Eq. (1) and putting $F_L/EA = f_L$ leads to

$$\left\{ \begin{array}{c} 1 \\ -e^{\lambda} \end{array} \right\} f_L = \frac{1}{N_E \delta L} \left[\left[\begin{array}{cc} 1 & -1 \\ -1 & 1 \end{array} \right] - k_L^2 \delta L^2/2 \left[\begin{array}{cc} 1 & 0 \\ 0 & 1 \end{array} \right] \right] \left\{ \begin{array}{c} 1 \\ e^{\lambda} \end{array} \right\} u_L \tag{5a}$$

but $N_E \delta L = 1$ so this can be expanded and rearranged into the form

$$\left[\begin{array}{cc} 1 - k_L^2 \delta L^2/2 - e^{\mu} & -1 \\ -1 - e^{\mu} - (k_L^2 \delta L^2/2) e^{\mu} & e^{\mu} \end{array} \right] \left\{ \begin{array}{c} u_L \\ f_L \end{array} \right\} = 0. \tag{5b}$$

Finding e^{μ} from this for a given value of $k_L \delta L$ actually constitutes a quadratic eigenvalue problem, easily solved in this simple case by expanding the determinant of the 2×2 coeffficient matrix and equating it to zero. This yields

$$e^{2\mu} - 2(1 - k_L^2 \delta L^2/2) e^{\mu} + 1 = 0$$

which has the alternative form $e^{\mu} - 2(1 - k_L^2 \delta L^2/2) + e^{-\mu} = 0$. Evidently

$$\cosh \mu = 1 - k_L^2 \delta L^2/2. \tag{6a}$$

Now introduce the non-dimensional frequency $\Omega = (\omega/c_L) \times$ unit length, which is numerically equal to k_L. Eq. (6a) then takes the form

$$\cosh\mu = 1 - \Omega^2/2N_E^2 \qquad (6b)$$

At low frequencies and wave numbers or with small values of δL, $\cosh\mu$ lies between ± 1. μ is then purely imaginary. Denote it now by $i\varepsilon$, so $\cos\varepsilon = 1 - k_L^2\delta L^2/2$. But $\cos\varepsilon = \sqrt{1-\sin^2\varepsilon}$, and if ε is small enough, $\sqrt{1-\sin^2\varepsilon} \approx 1 - \varepsilon^2/2$. Under these conditions $\varepsilon^2 \approx k_L^2\delta L^2$ and $\varepsilon \approx k_L\delta L$ to an increasing degree of accuracy as δL decreases.

Now ε represents the phase difference between the displacements (and the forces) at corresponding ends of adjacent elements. When there are N_E (= $1/\delta L$) elements per unit length of the bar, the total phase change associated with the wave across the unit length is $N_E\varepsilon = \varepsilon/\delta L \approx k_L$ which, by definition, is the correct wave number for longitudinal wave motion in the bar. It follows that the accuracy of the approximate finite element calculation increases as δL decreases, unless computer rounding errors intervene..

If δL or the frequency are large enough, $\cosh\lambda < -1$, in which case μ is complex of the form $\mu_{real} + i\pi$ and μ_{real} represents the exponential decay or growth rate of the wave motion across a single element. Such evanescent waves cannot exist in the ideal uniform bar, but the finite element model erroneously predicts them because the strain within each finite element is assumed to be uniform and the bar mass is lumped at the discrete intervals of δL. The whole finite element model of the bar constitutes a periodic mass-spring system along which waves can only propagate without decay at frequencies below the natural frequency of a single massless spring which has half an element mass at each of its ends. Above this frequency (which is the 'cut-off frequency' of propagating wave motion in the periodic system) any motion decays exponentially from element to element. Over the N_E elements in the modelled bar of unit length, the wave amplitude decays to $\exp(N_E\mu_{real})$ times its initial value.

2.2 Wave numbers calculated by the FE-PS method

Calculated values of the complex wave number for a FE model with one element per unit length are shown plotted against the non-dimensional Ω on Figure 2 ($N_E = 1/\delta L = 1$). For clarity, the

real and imaginary parts of μ are plotted in the positive and negative domains respectively, so the decay index is presented in the positive domain.

The calculated values are within 1% of the correct values at frequencies below $\Omega = 0.48$ and the error decreases below this as Ω decreases. The decay index emerges from zero at the ND frequency $\Omega = 2$ which is the wave cut-off frequency for the simple mass-spring periodic system. Above this frequency the FE-computed wave number remains constant at $\pm\pi$ whereas the correct value increases, being numerically equal to Ω.

Similarities between the curve for $N_E = 1$ and those for higher values of N_E are seen in Figure 3. All the curves have the same general shape but their actual values and the frequencies at which they occur have all increased. It can be formally proved that the curves for any value of N_E can be found by multiplying those for $N_E = 1$ (both the real and imaginary parts) and the frequency by N_E.

The curves for $N_E = 1000$ are indistinguishable from those of the exact values for the ideal bar. However, at the higher end of the wide frequency range covered, the assumptions break down on which the elementary 'exact' theory are based. The presented values are therefore inapplicable to real uniform bars except in the low frequency range. However, they do show that the FE-PS (Finite Element- Periodic Structure) method of calculation yields results which are as close to the correct ones as desired, and this is accomplished simply by making N_E large enough. Most importantly, the computation time is independent of the value of N_E.

2.3 The dynamic stiffness of a semi-infinite uniform bar

Consider now the ideal semi-infinite bar in the positive x-domain. The exact theory for this bar shows its dynamic stiffness (F/u) at its free end to be simply $-ik_L EA$. This corresponds to a single wave propagating freely along the bar in the positive x-direction. When a positive-going wave travels through the FE model of the bar, the corresponding dynamic stiffness at the left hand end of any element is F_L/u_L from Eq. (2) with u_R set equal to $e^{\mu}u_L$. This yields

$\frac{F_L}{u_L} = \frac{EA}{\delta L}\{1 - e^{\mu} - k_L^2 \delta L^2/2\}$ but since $1 - k_L^2/2N_E^2 = \cosh\mu$ (Eq.(6b)) it simplifies to

$$\frac{F_L}{u_L} = EA.N_E \sinh\mu \quad \text{or} \quad \frac{f_L}{u_L} = N_E \sinh\mu \tag{7}$$

Figure 4 compares the values obtained from Eq. (7) for different values of N_E and frequency. At low frequencies, the dynamic stiffness is imaginary for all values of N_E. These all drop sharply to zero at the cut-off frequency appropriate to the particular value of N_E and above these frequencies they all become real. The curve for $N_E = 1000$ is indistiguishable from the curve for the exact values.

2.4 The frequency response of a finite bar excited at one end

Expressions for this will be derived in two different ways. The first is the quickest for this particular simple uniform bar while the second is a matrix formulation which introduces the matrix method required for more complicated structural systems.

The finite bar will be taken to be of unit length. At its left hand end it is excited by a harmonic force which generates a positive-going wave which has the complex amplitude u_P at that end and has the (complex) wave number $N_E\mu_P$. At the right hand end its complex amplitude becomes $u_P e^{N_E\mu_P}$. It is reflected at that end and returns as a negative-going wave with the wave number $N_E\mu_N$. Denote its amplitude at the left hand end by u_N so its amplitude at the right hand end must be $u_N e^{N_E\mu_N}$. Since the two waves constitute the pair of opposite-going waves, $\mu_N = -\mu_P$. The ND forces, f_P, f_N, acting on the bar corresponding to each of these waves are given by Eq. (7), so at the left hand end they are $u_P N_E \sinh\mu_P$ and $u_N N_E \sinh\mu_N$. At the right hand end they are $u_P N_E e^{N_E\mu_P} \sinh\mu_P$ and $u_N N_E e^{N_E\mu_N} \sinh\mu_N$.

The two waves combine at each end of the bar to satisfy the two boundary conditions. Suppose the left hand end is excited by the external harmonic force of amplitude $F_{ext} = EAf_{ext}$ while the right hand end is free. The total force from the two waves at the free right hand end must be zero so $u_P e^{N_E\mu_P} \sinh\mu_P + u_N e^{N_E\mu_N} \sinh\mu_N = 0$. $u_P N_E e^{N_E\mu_P}$. Since $\mu_N = -\mu_P$ it follows that

$$u_N = u_P e^{2N_E\mu_P}. \tag{8}$$

The total force from the two waves at the forced left-hand end is equal to the applied force F_{ext},. Its non-dimensional value, f_{ext}, is therefore given by

$$f_{ext} = N_E(u_P \sinh\mu_P + u_N \sinh_N) = N_E u_P(1 - e^{2N_E\mu_P})\sinh\mu_P = N_E u_P \frac{2\sinh N_E\mu_P}{e^{N_E\mu_P}} \sinh\mu_P. \tag{9}$$

Hence $u_P = f_{ext}\frac{e^{-N_E\mu_P}}{2N_E \sinh N_E\mu_P \sinh\mu_P}$. (10)

The total displacement at the left hand end is $u_L = u_P + u_N = u_P(1 + e^{2N_E\lambda_P})$ so

$$\frac{u_L}{f_{ext}} = \frac{1}{N_E}\frac{\cosh N_E\lambda_P}{\sinh N_E\lambda_P \sinh\lambda_P} = \frac{1}{N_E \sinh\lambda_P}\coth N_E\lambda_P \tag{11}$$

The exact expression for this (derived from the flexural wave equation) is $(\coth k_L)/k_L$. Eq. (11) approaches this as N_E gets very large and μ_P becomes very small, because $N_E\mu_P$ approaches k_L .

Figures 5a,b shows the the direct receptance of the bar (the response amplitude per unit exciting force at the forced end) as calculated from Eq. (11) for different values of N_E over two ND frequency ranges, Ω = 0 -10 and 90 - 100. The figures demonstrate the well-known fact that increasing the number of elements per unit length improves the accuracy of calculation. In the (unreasonably) high frequency range of 90 to 100, 50 elements per unit length yield unacceptable values, while the results from 1000 elements are almost indistinguishable from the exact values. Once again, it must emphasised that it takes no longer by the FE-PS method to calculate for 1000 elements (or for 10^{12} elements, for that matter!) than it does for 1, 2 or 50 elements.

The alternative matrix formulation for the response calculation proceeds as follows. The total end displacements u_L and u_R of the finite bar are related to the two wave amplitudes, u_P and u_N, by

$$\begin{Bmatrix} u_L \\ u_R \end{Bmatrix} = \begin{bmatrix} 1 & 1 \\ e^{N_E\lambda_P} & e^{N_E\lambda_N} \end{bmatrix} \begin{Bmatrix} u_P \\ u_N \end{Bmatrix} \quad \text{so} \quad \begin{Bmatrix} u_P \\ u_N \end{Bmatrix} = \begin{bmatrix} 1 & 1 \\ e^{N_E\lambda_P} & e^{N_E\lambda_N} \end{bmatrix}^{-1} \begin{Bmatrix} u_L \\ u_R \end{Bmatrix} \tag{12}$$

The forces associated with each wave at the left and right hand ends are, respectively,

$$\begin{Bmatrix} f_P \\ f_N \end{Bmatrix}_L = N_E \begin{bmatrix} \sinh\lambda_P & 0 \\ 0 & \sinh\lambda_N \end{bmatrix} \begin{Bmatrix} u_P \\ u_N \end{Bmatrix} \quad \text{(from Eq.(7))} \tag{13a}$$

and

$$\begin{Bmatrix} f_P \\ f_N \end{Bmatrix}_R = N_E \begin{bmatrix} \sinh\lambda_P & 0 \\ 0 & \sinh\lambda_N \end{bmatrix} \begin{bmatrix} e^{N_E\lambda_P} & 0 \\ 0 & e^{N_E\lambda_N} \end{bmatrix} \begin{Bmatrix} u_P \\ u_N \end{Bmatrix} \tag{13b}$$

The total forces acting at each end are given by

$$\begin{Bmatrix} f_L \\ f_R \end{Bmatrix} = N_E \begin{bmatrix} 1 & 1 \\ e^{N_E\mu_P} & e^{N_E\mu_N} \end{bmatrix} \begin{bmatrix} \sinh\mu_P & 0 \\ 0 & \sinh\mu_N \end{bmatrix} \begin{Bmatrix} u_P \\ u_N \end{Bmatrix}$$

$$= N_E \begin{bmatrix} 1 & 1 \\ e^{N_E\mu_P} & e^{N_E\mu_N} \end{bmatrix} \begin{bmatrix} \sinh\mu_P & 0 \\ 0 & \sinh\mu_N \end{bmatrix} \begin{bmatrix} 1 & 1 \\ e^{N_E\mu_P} & e^{N_E\mu_N} \end{bmatrix}^{-1} \begin{Bmatrix} u_L \\ u_R \end{Bmatrix} \tag{14}$$

Now put $\mu_N = -\mu_P = \mu$. The non-dimensional dynamic stiffness matrix of the whole finite system of N_E elements is then seen to be

$$DS_{NE} = N_E \begin{bmatrix} 1 & 1 \\ e^{N_E\mu} & e^{-N_E\mu} \end{bmatrix} \begin{bmatrix} \sinh\mu & 0 \\ 0 & -\sinh\mu \end{bmatrix} \begin{bmatrix} 1 & 1 \\ e^{N_E\mu} & e^{-N_E\mu} \end{bmatrix}^{-1} \tag{15}$$

The displacements at the two ends of the system are therefore given by

$$\begin{Bmatrix} u_L \\ u_R \end{Bmatrix} = \frac{1}{N_E} \left[\begin{bmatrix} 1 & 1 \\ e^{N_E\mu} & e^{-N_E\mu} \end{bmatrix} \begin{bmatrix} \sinh\mu & 0 \\ 0 & -\sinh\mu \end{bmatrix} \begin{bmatrix} 1 & 1 \\ e^{N_E\mu} & e^{-N_E\mu} \end{bmatrix}^{-1} \right]^{-1} \begin{Bmatrix} f_L \\ f_R \end{Bmatrix} \tag{16}$$

Expanding this matrix product leads (as it should) to the same expressions for the displacements as derived by the first method. In more complicated structural systems than the uniform bar, the

matrices are of higher order (perhaps of much higher order) and such expansion is impracticable. However, computer calculations based on them present no undue problem.

3. DEVELOPMENT OF THE METHOD FOR MULTI-COUPLED SYSTEMS

3.1 THE GENERAL APPROACH

Consider the rectangular array of finite elements of Figure 6(a) which has N_T elements in each stack across the array (i.e. in the transverse y-direction) which need not be identical. There are N_L identical stacks per unit length along the array in the longitudinal x-direction. These are joined identically, side-by-side through n_C coupling co-ordinates and n_C coupling forces or moments. The whole system is therefore periodic in the longitudinal direction. It is required to find the dynamic stiffness and receptance matrices relating the displacements at any stack location to the externally applied forces on the system or to the internal forces acting between any other stack location. These locations may be separated by very many stacks, the feature which can lead to very long calculations by the normal finite element method. The methods of periodic structure analysis reduce the calculation dramatically, because the two matrices can be found by analysing just one stack of N_T elements.

It has long been known [1,4] that any harmonic motion through a periodic structure with n_c coupling co-ordinates can be decomposed into $2n_C$ ($=J$) harmonic waves, each of which has a characteristic propagation constant and a spatially non-sinusoidal wave-form. The $2n_C$ propagation constants occur in equal and opposite pairs which, in an undamped system, may be purely real, generally complex or purely imaginary. The purely imaginary values are associated with energy-propagating wave motions whose amplitudes do not change with distance from the source. Both the real and generally complex values are associated with evanescent wave motions which decay or grow with distance from the source but are not associated with energy transmission.

All of these propagation constants and wave motions are determined by the methods of periodic structure theory from an analysis of a single stack of N_T elements. An imaginary propagation constant represents the change of phase of a wave over the x-wise length of the element,

while the real or generally-complex constant represents the exponential decay index of the wave over that length. Multiplying these propagation constants by the number of element-stacks per unit length of the system yields the actual wave number or decay index of the wave.

Each wave is associated with a unique vector of cross-sectional distortion. This is found, together with the propagation constants, from an analysis of the dynamic stiffness matrix of just one complete stack of N_T elements. The dynamic stiffness or receptance matrices of both infinite and finite lengthwise arrays of such elements are then derived from all of these quantities.

3.2 The relationship between the wave numbers and the stack dynamic stiffness matrix

Consider the 'reference' stack (identified as stack 1) and its nodal displacements and forces as shown in Figure 6(b). Denote the displacements along its left-hand side by the column matrix $\{q_L\}_1$ and those along its right-hand side by $\{q_R\}_1$. The forces acting at these co-ordinates are $\{F_L\}_1$ and $\{F_R\}_1$. Define the complete displacement and force vectors for stack 1 by

$$\{q\}_1 = \begin{Bmatrix} \{q_L\}_1 \\ \{q_R\}_1 \end{Bmatrix} \quad \text{and} \quad \{F\}_1 = \begin{Bmatrix} \{F_L\}_1 \\ \{F_R\}_1 \end{Bmatrix} \tag{17a,b}$$

Standard finite element methods yield the dynamic stiffness matrix $[D]$ which relates these two vectors for many different structural systems (e.g. beams, plates, frameworks etc.). Since each stack of elements in the system is the same, D requires no subscript as it applies to every stack in the whole system.

It is convenient to partition D in the following manner:

$$\begin{Bmatrix} \{F_L\}_1 \\ \{F_R\}_1 \end{Bmatrix} = \begin{bmatrix} D_{LL} & D_{LR} \\ D_{RL} & D_{RR} \end{bmatrix} \begin{Bmatrix} \{q_L\}_1 \\ \{q_R\}_1 \end{Bmatrix} \tag{18}$$

Consider now the wave which propagates with propagation constant μ. The displacement and force vectors along the left-hand side of the next stack of elements (stack 2) are given simply by the Floquet relationship

$$\{q_L\}_2 = \{q_L\}_1 e^{\mu} \quad \text{and} \quad \{F_L\}_2 = \{F_L\}_1 e^{\mu} \tag{19a,b}$$

Continuity of displacement and equilibrium of forces between stacks 1 and 2 require that $\{q_R\}_1 = \{q_L\}_2$ and $\{F_R\}_1 = -\{F_L\}_2$. Hence

$$\{q_R\}_1 = \{q_L\}_1 e^{\mu} \quad \text{and} \quad \{F_R\}_1 = -\{F_L\}_1 e^{\mu} \tag{20a,b}$$

Substitute these into Eq. s (17) to obtain the two equations

$$\{F_L\}_1 = [D_{LL} + D_{LR} e^{\mu}]\{q_L\}_1 \tag{21a}$$

$$\text{and } -\{F_L\}_1 e^{\mu} = [D_{RL} + D_{RR} e^{\mu}]\{q_L\}_1 \quad \text{or} \quad \{F_L\}_1 = -[D_{RL} e^{-\mu} + D_{RR}]\{q_L\}_1 \tag{21b}$$

Equating the first and last of these three leads to

$$[D_{RL} e^{-\mu} + D_{LL} + D_{RR} + D_{LR} e^{\mu}]\{q_L\}_1 = 0 \quad \text{or} \quad [D_{RL} + (D_{LL} + D_{RR}) e^{\mu} + D_{LR} e^{2\mu}]\{q_L\}_1 = 0 \tag{22}$$

which is recognised as a quadratic eigenvalue equation for e^{μ}. $2N_T$ different eigenvalues are obtained and occur in reciprocal pairs. The corresponding values of μ therefore occur in positive and negative pairs.

Now μ represents the phase change or exponential decay index of a wave motion across a single stack. As there are N_L stacks in a unit length of the whole system, it follows that

$$\text{Wave number} = N_L \mu \tag{23}$$

Symmetry of the D matrix means that $D_{RL} = D_{LR}^T$ and this can be used to re-express Eq. (22) in terms of $\sinh\mu$ and $\cosh\mu$. Thompson [10] has shown how it can be reduced to a simpler linear eigenvalue equation in $\cosh\mu$.

3.3 Displacements and forces at different points in a stack array

A general free harmonic motion in the array of N_L stacks consists of all the waves with the above wave numbers. Associated with the jth eigenvalue μ_j is the eigenvector $\{q_L\}_j$ to be denoted (in its normalised form) by θ_j. Corresponding to this is the normalised force vector ϕ_j, which from Eq. (18) is seen to be given by

$$\{\phi_j\} = [D_{LL} + D_{LR}e^{\mu_j}]\{\theta_j\}. \tag{24}$$

Let the generalised co-ordinate of wave vector θ_j at the left hand side of the first (i.e. the reference) stack be ψ_j, so the actual displacements and forces along this left hand side corresponding to this are $\{q_L\}_1 = \{\theta_j\}\psi_j$ and $\{F_L\}_1 = \{\phi_j\}\psi_j$. respectively. The total displacements and forces on the left-hand side of the stack when all J waves are present in the total motion are given by

$$\{q_L\}_1 = \sum_{j=1}^{J} \theta_j\psi_j \qquad \text{and} \qquad \{F_L\}_1 = \sum_{j=1}^{J} \phi_j\psi_j \quad . \tag{25a,b}$$

All J waves will be present in a general motion so the positive and negative wave of each wave pair must be included.

Along the left-hand side of the next stack of elements in the system (i.e. to the right, stack 2) the amplitude of each of these terms is multiplied by e^{μ_j}. For continuity and equilibrium at the junction of stacks 1 and 2, the displacements and forces along the right-hand side of stack 1 must be given by

$$\{q_R\}_1 = \{q_L\}_2 = \sum_{j=1}^{J} e^{\mu_j}\theta_j\psi_j \qquad \text{and} \qquad \{F_R\}_1 = -\{F_L\}_2 = -\sum_{j=1}^{J} e^{\mu_j}\phi_j\psi_j \tag{26a,b}$$

Note the negative sign in front of $\{F_L\}_2$. It now follows that the displacements and forces along the right-hand side of stack N_L in the whole periodic array are given by

$$\{\boldsymbol{q}_R\}_{N_L} = \sum_{j=1}^{J} \boldsymbol{e}^{N_L\mu_j}\theta_j\psi_j \quad \text{and} \quad \{\boldsymbol{F}_R\}_{N_L} = -\sum_{j=1}^{J} \boldsymbol{e}^{N_L\mu_j}\phi_j\psi_j \tag{27a,b}$$

These summations can all be expressed in the following matrix forms.

$$\{q_L\}_1 = \sum_{j=1}^{J} \theta_j \psi_j = \begin{bmatrix} \theta_{1,1} & \theta_{2,1} & . & . & \theta_{J,1} \\ \theta_{1,2} & \theta_{2,2} & . & . & \theta_{J,2} \\ . & . & . & . & . \\ . & . & . & . & . \\ \theta_{1,J} & \theta_{2,J} & . & . & \theta_{J,J} \end{bmatrix} \begin{Bmatrix} \psi_1 \\ \psi_2 \\ . \\ . \\ \psi_J \end{Bmatrix} = [\Theta]\{\Psi\} \tag{28a}$$

$$\{F_L\}_1 = \sum_{j=1}^{J} \phi_j \psi_j = \begin{bmatrix} \phi_{1,1} & \phi_{2,1} & . & . & \phi_{J,1} \\ \phi_{1,2} & \phi_{2,2} & . & . & \phi_{J,2} \\ . & . & . & . & . \\ . & . & . & . & . \\ \phi_{1,J} & \phi_{2,J} & . & . & \phi_{J,J} \end{bmatrix} \begin{Bmatrix} \psi_1 \\ \psi_2 \\ . \\ . \\ \psi_J \end{Bmatrix} = [\Phi]\{\Psi\} \tag{28b}$$

$$\{q_L\}_{N_L} = \sum_{j=1}^{J} e^{N_L \mu_j} \theta_j \psi_j = \begin{bmatrix} \theta_{1,1} & \theta_{2,1} & . & . & \theta_{J,1} \\ \theta_{1,2} & \theta_{2,2} & . & . & \theta_{J,2} \\ . & . & . & . & . \\ . & . & . & . & . \\ \theta_{1,J} & \theta_{2,J} & . & . & \theta_{J,J} \end{bmatrix} \begin{bmatrix} e^{N_L \mu_1} & 0 & 0 & 0 & 0 \\ 0 & e^{N_L \mu_2} & 0 & 0 & 0 \\ 0 & 0 & . & . & 0 \\ 0 & 0 & . & . & 0 \\ 0 & 0 & 0 & 0 & e^{N_L \mu_J} \end{bmatrix} \begin{Bmatrix} \psi_1 \\ \psi_2 \\ . \\ . \\ \psi_J \end{Bmatrix}$$

$$= [\Theta][E^{\mu}]^{N_L}\{\Psi\} \tag{28c}$$

$$\{F_R\}_{N_L} = -\sum_{j=1}^{J} e^{N_L \mu_j} \phi_j \psi_j = -\begin{bmatrix} \phi_{1,1} & \phi_{2,1} & . & . & \phi_{J,1} \\ \phi_{1,2} & \phi_{2,2} & . & . & \phi_{J,2} \\ . & . & . & . & . \\ . & . & . & . & . \\ \phi_{1,J} & \phi_{2,J} & . & . & \phi_{J,J} \end{bmatrix} \begin{bmatrix} e^{N_L \mu_1} & 0 & 0 & 0 & 0 \\ 0 & e^{N_L \mu_2} & 0 & 0 & 0 \\ 0 & 0 & . & . & 0 \\ 0 & 0 & . & . & 0 \\ 0 & 0 & 0 & 0 & e^{N_L \mu_J} \end{bmatrix} \begin{Bmatrix} \psi_1 \\ \psi_2 \\ . \\ . \\ \psi_J \end{Bmatrix}$$

$$= -[\Phi][E^{\mu}]^{N_L}\{\Psi\} \tag{28d}$$

where $$[E^{\mu}] = \begin{bmatrix} e^{\mu_1} & 0 & 0 & 0 & 0 \\ 0 & e^{\mu_2} & 0 & 0 & 0 \\ 0 & 0 & . & . & 0 \\ 0 & 0 & . & . & 0 \\ 0 & 0 & 0 & 0 & e^{\mu_J} \end{bmatrix} \quad (29)$$

$[\Theta]$ and $[\Phi]$ are matrices of the displacement vectors and corresponding force vectors respectively, of order $n_C \times 2n_C$. $\{\Psi\}$ is a column matrix of the $2n_C$ ψ_j's. The above matrix equations will now be used to investigate specific cases of forced response of both infinite and finite arrays.

4. THE RESPONSE OF PERIODIC STACK ARRAYS TO APPLIED HARMONIC FORCES

4.1 THE SEMI-INFINITE SYSTEM EXCITED AT THE FINITE END

Consider the system extending indefinitely to the right and excited at the left-hand end of stack 1 by the known set of forces/moments $\{F_L\}_1$. The displacements $\{q_L\}_1$ are unspecified, no other displacements or forces being specified elsewhere in the system. In the absence of a termination or any discontinuity to the right of stack 1 there are no backward reflected waves towards the source of excitation so the only admissible wave motions in the system are those which propagate or decay away from the source. The displacement(s) at any other point in the system can be found when the values of the ψ's have been determined which pertain to the positive-going waves, i.e. those with μ's with negative real parts or negative purely imaginary parts. There are only n_c of these with their corresponding wave vectors $\{\theta\}$ and $\{\phi\}$. Their ψ's satisfy the known set of forces at the source constituted by the given n_c values $\{F_L\}_1$. Hence, from Eq. (24b) one obtains

$$\{\Psi\} = [\Phi]^{-1}\{F_L\}_1 \quad (30)$$

where $[\Phi]$ is now an invertible square matrix of positive-going wave vectors of order $n_c \times n_c$.

The displacements and forces in the system at junction N are given as in Eq. (27c) by

$$\{q_R\}_N = [\Theta][E^\mu]^N\{\Psi\} = [\Theta][E^\mu]^N[\Phi]^{-1}\{F_L\}_1 \tag{31}$$

and

$$\{F_R\}_N = -[\Phi][E^\mu]^N\{\Psi\} = -[\Phi][E^\mu]^N[\Phi]^{-1}\{F_L\}_1 \tag{32}$$

Now consider the semi-infinite system which extends indefinitely to the left (i.e. to $-\infty$). The only waves participating in the total motion are those which propagate or decay in the negative direction away from the source, so the ψ's to be found are those associated with values of μ with positive real parts or positive purely imaginary parts. To distinguish these quantities from those of the 'right-hand' semi-infinite system, a minus sign will be added to their symbols as a prefixed index, i.e. ${}^-\Psi, {}^-\psi_j, {}^-\theta_j, {}^-\mu_j, {}^-\Theta, {}^-\Phi$.

The displacement vector at the right-hand (excited) end of the system is $\{{}^-q_R\}_1$ and the total displacements and acting forces at that end are

$$\{{}^-q_R\}_1 = \sum_{j=1}^{J} {}^-\theta_j\, {}^-\psi_j = [{}^-\Theta]\{{}^-\Psi\} \quad \text{and} \quad \{{}^-F_R\}_1 = -\sum_{j=1}^{J} {}^-\phi_j\, {}^-\psi_j = -[{}^-\Phi]\{{}^-\Psi\} \tag{33a,b}$$

The ${}^-\theta_j$'s and ${}^-\phi_j$'s to be used in these would be determined in the same eigenvalue calculation used to find the values required for the right-hand semi-infinite system. As the finite end of the left-hand semi- inifinite system is at the right-hand side of a stack, the negative sign must appear in the expression for $\{{}^-F_R\}_1$.

$[{}^-\Phi]$ is an invertible square matrix so

$$\{{}^-\Psi\} = -[{}^-\Phi]^{-1}\{{}^-F_R\}_1 \tag{34}$$

With J specified values of the F_R's , the J values of ψ_j can now be determined. At the junction N stacks to the left of stack 1 the displacements and forces at junction N are now given by Eq. (27c,d) (as for the right-hand semi-infinite system). Hence

$$\{^{-}q_R\}_N = [^{-}\Theta][E^{-\mu}]^N\{^{-}\Psi\} \qquad \text{and} \qquad \{^{-}F_R\}_N = -[^{-}\Phi][E^{-\mu}]^N\{^{-}\Psi\}. \tag{35a,b}$$

4.2 The doubly-infinite system excited at a single junction

The system now extends to $N_E = \pm\infty$ on either side of the loaded junction. On either side of the junction the system may be regarded as semi-infinite. At their junction, the total displacements in each system must be identical and the total force from each system at corresponding co-ordinates must equal the local externally applied force. Some of the displacements may be found to be zero, but we cannot say *a priori* which ones these will be. Expressions from the previous section for the semi-infinite systems will be used to set up the equations for this infinite system.

Identify the quantities relating to the right-hand system by a positive prefixed index, i.e. by $^{+}\Psi, ^{+}\psi_j, ^{+}\theta_j, ^{+}\mu_j$ etc. Equate the displacements at the junctions of the left-hand and right-hand systems, using Eq. s (33a, 35a) to yield

$$\{^{+}q_R\}_1 = [^{+}\Theta]\{^{+}\Psi\} = \{^{-}q_L\}_1 = [^{-}\Theta]\{^{-}\Psi\}$$

$$\text{so} \quad [^{+}\Theta]\{^{+}\Psi\} - [^{-}\Theta]\{^{-}\Psi\} = 0. \tag{36}$$

Equate the sum of the forces in the two systems at the junction to the externally applied forces, using Eq. s (33b, 35b). This yields

$$\{^{+}F_L\}_1 + \{^{-}F_R\}_1 = [^{+}\Phi]\{^{+}\Psi\} - [^{-}\Phi]\{^{-}\Psi\} = \{F_{EXT}\} \tag{37}$$

Now combine these two Eq. s (36, 37) into the single equation for $\{^{+}\Psi\}$ and $\{^{-}\Psi\}$:

$$\begin{bmatrix} ^{+}\Theta & -^{-}\Theta \\ ^{+}\Phi & -^{-}\Phi \end{bmatrix}\begin{Bmatrix} ^{+}\Psi \\ ^{-}\Psi \end{Bmatrix} = \begin{Bmatrix} 0 \\ F_{EXT} \end{Bmatrix} \tag{38}$$

$$\text{so} \qquad \begin{Bmatrix} ^{+}\Psi \\ ^{-}\Psi \end{Bmatrix} = \begin{bmatrix} ^{+}\Theta & -^{-}\Theta \\ ^{+}\Phi & -^{-}\Phi \end{bmatrix}^{-1}\begin{Bmatrix} 0 \\ F_{EXT} \end{Bmatrix} \tag{39}$$

From the ${}^{+}\Psi$ and ${}^{-}\Psi$ values obtained from this and by using Eq. s (33) and (35) one can now find the displacements and forces at any point in either part of the infinite system.

4.3 The finite system of N_L stacks excited at its ends

The matrix equations for $\{q_L\}$ and $\{q_R\}$, $\{F_L\}$ and $F_R\}$ for the finite stack can be stacked to relate the whole set of end-displacements and end-forces to $\{\Psi\}$. In this way, we get

$$\begin{Bmatrix} \{q_L\}_1 \\ \{q_R\}_{NL} \end{Bmatrix} = \begin{bmatrix} [\Theta] \\ [\Theta][E^{\mu}]^{N_L} \end{bmatrix} \{\Psi\} \quad \text{and} \quad \begin{Bmatrix} \{F_L\}_1 \\ \{F_R\}_{NL} \end{Bmatrix} = \begin{bmatrix} [\Phi] \\ -[\Phi][E^{\mu}]^{N_L} \end{bmatrix} \{\Psi\} \qquad (40a,b)$$

in which the matrices containing $[\Theta]$ and $[\Phi]$ are square and invertible, so

$$\{\Psi\} = \begin{bmatrix} [\Theta] \\ [\Theta][E^{\mu}]^{N_L} \end{bmatrix}^{-1} \begin{Bmatrix} \{q_L\}_1 \\ \{q_R\}_{N_L} \end{Bmatrix} \text{ and } \{\Psi\} = \begin{bmatrix} [\Phi] \\ -[\Phi][E^{\mu}]^{N_L} \end{bmatrix}^{-1} \begin{Bmatrix} \{F_L\}_1 \\ \{F_R\}_{N_L} \end{Bmatrix} \qquad (41a,b)$$

Altogether these constitute $4N_L$ equations for the $2N_L$ values of ψ. To start with, the only usable ones are those $2N_L$ which specify known displacements or forces at the extreme ends, i.e. they express the boundary conditions. However, they constitute sufficient equations to allow $\{\Psi\}$ to be determined. From the remaining $2N_L$ equations, all the unknown displacements or forces at the extreme ends can be found.

Consider now the system which is excited by known forces at the left-hand and/or the right-hand end, but the end displacements are not otherwise constrained. $\{F_L\}_1$ and $\{F_R\}_{N_L}$ are therefore known, but $\{q_L\}_1$ and $\{q_R\}_{N_L}$ are all unknown. Hence

$$\{\Psi\} = \begin{bmatrix} [\Phi] \\ -[\Phi][E^{\mu}]^{N_L} \end{bmatrix}^{-1} \begin{Bmatrix} \{F_L\}_1 \\ \{F_R\}_{N_L} \end{Bmatrix} \quad \text{and} \qquad (42)$$

$$\begin{Bmatrix} \{q_L\}_1 \\ \{q_R\}_{N_L} \end{Bmatrix} = \begin{bmatrix} \Theta \\ \Theta[E^{\mu}]^{N_L} \end{bmatrix} \{\Psi\} = \begin{bmatrix} \Theta \\ \Theta[E^{\mu}]^{N_L} \end{bmatrix} \begin{bmatrix} [\Phi] \\ -[\Phi][E^{\mu}]^{N_L} \end{bmatrix}^{-1} \begin{Bmatrix} \{F_L\}_1 \\ \{F_R\}_{N_L} \end{Bmatrix} \qquad (43)$$

The overall receptance matrix for the whole system is therefore

$$a_{1,NL} = \begin{bmatrix} \Theta \\ \Theta[E^{\mu}]^{N_L} \end{bmatrix} \begin{bmatrix} [\Phi] \\ -[\Phi][E^{\mu}]^{N_L} \end{bmatrix}^{-1} \tag{44}$$

Computational difficulties arise with this when the terms in E^{μ} with positive exponents are raised to a large enough power of N_L to cause computer overflow. This must be circumvented by splitting Ψ into its positive and negative-going components, Ψ_+ and Ψ_+, with Ψ_- representing magnitudes at the right-hand end of the waves with positive μ's while Ψ_+ still represents magnitudes at the left-hand end of the waves with negative μ's. The total motion at the two ends is now

$$\{q_L\} = \Theta_+\Psi_+ + \Theta_-e^{-N_L\mu}\Psi_- \quad \text{and} \quad \{q_R\} = \Theta_+e^{-N_L\mu}\Psi_+ + \Theta_-\Psi_- \tag{45a,b}$$

Only the N_L positive values of μ are are now used[1]. Altogether, the end displacements are given by

$$\begin{Bmatrix} q_L \\ q_R \end{Bmatrix} = \begin{bmatrix} \Theta_+ & \Theta_-e^{-NL\mu} \\ \Theta_+e^{-NL\mu} & \Theta_- \end{bmatrix} \begin{Bmatrix} \Psi_+ \\ \Psi_- \end{Bmatrix} \tag{46}$$

The total forces at the ends associated with this motion are expressed in similar form by

$$\begin{Bmatrix} F_L \\ F_R \end{Bmatrix} = \begin{bmatrix} \Phi_+ & \Phi_-e^{-NL\mu} \\ -\Phi_+e^{-NL\mu} & -\Phi_- \end{bmatrix} \begin{Bmatrix} \Psi_+ \\ \Psi_- \end{Bmatrix} \tag{47}$$

so

$$\begin{Bmatrix} \Psi_+ \\ \Psi_- \end{Bmatrix} = \begin{bmatrix} \Phi_+ & \Phi_-e^{-NL\mu} \\ -\Phi_+e^{-NL\mu} & -\Phi_- \end{bmatrix}^{-1} \begin{Bmatrix} F_L \\ F_R \end{Bmatrix} \tag{48}$$

[1] In effect, this formulation considers the waves with positive μ's to be initiated at the right hand end of the system whereas those with negative μ's are initiated at the left hand end.

Hence

$$\begin{Bmatrix} q_L \\ q_R \end{Bmatrix} = \begin{bmatrix} \Theta_+ & \Theta_- e^{-NL\mu} \\ \Theta_+ e^{-NL\mu} & \Theta_- \end{bmatrix} \begin{bmatrix} \Phi_+ & \Phi_- e^{-NL\mu} \\ -\Phi_+ e^{-NL\mu} & -\Phi_- \end{bmatrix}^{-1} \begin{Bmatrix} F_L \\ F_R \end{Bmatrix} \tag{49}$$

4.4 The system with one end fully constrained

- Consider next the system whose right hand end is rigidly fixed, while a known set of forces acts at the left hand end. $\{q_R\}_{N_L}$ is now zero so

$$\begin{Bmatrix} \{F_L\}_1 \\ \{q_R\}_{N_L} = 0 \end{Bmatrix} = \begin{bmatrix} [\Phi] \\ [\Theta][E^\mu]^{N_L} \end{bmatrix} \{\Psi\} \quad \text{and} \quad \{\Psi\} = \begin{bmatrix} [\Phi] \\ [\Theta][E^\mu]^{N_L} \end{bmatrix}^{-1} \begin{Bmatrix} \{F_L\}_1 \\ 0 \end{Bmatrix} \tag{50a,b}$$

The unknown boundary displacements and forces are now given by

$$\begin{Bmatrix} \{q_L\}_1 \\ \{F_R\}_{NL} \end{Bmatrix} = \begin{bmatrix} [\Theta] \\ -[\Phi][E^\mu]^{N_L} \end{bmatrix} \{\Psi\} = \begin{bmatrix} [\Theta] \\ -[\Phi][E^\mu]^{N_L} \end{bmatrix} \begin{bmatrix} [\Phi] \\ [\Theta][E^\mu]^{N_L} \end{bmatrix}^{-1} \begin{Bmatrix} \{F_L\}_1 \\ 0 \end{Bmatrix} \tag{51}$$

Once $\{\Psi\}$ has been evaluated, the displacements or forces at any other point within the whole periodic system can be found. In particular, the displacement co-ordinate k at the left hand end of stack N_J is given by

$$q_{Lk,N_J} = \begin{bmatrix} \theta_{1,k} & \theta_{2,k} & \ldots & \theta_{J,k} \end{bmatrix} [E^\mu]^{N_J} \{\Psi\} \tag{52a}$$

and the force acting at the same co-ordinate is

$$[F_L]_{k,N_J} = \begin{bmatrix} \phi_{1,k} & \phi_{2,k} & \ldots & \phi_{J,k} \end{bmatrix} [E^\mu]^{N_J} \{\Psi\} \tag{52b}$$

4.5 THE FINITE SYSTEM EXCITED AT A SINGLE INTERMEDIATE JUNCTION

From the excited junction to the left- and right-hand ends there are N_{FL} and N_{FR} stacks respectively, so the total number of stacks in the whole system is $N_L = N_{FL} + N_{FR}$. There are therefore $J\,(=2n_c)$ different waves of unknown amplitude to the left of the excited junction and another (different) set of J waves to the right of the excited junction, i.e. there are $2J$ unknowns altogether. The computational problem, however, may be solved by a method (using some of the above equations) which involves only J unknowns at a time. The method has often been used in solving uniform-beam vibration problems by utilizing known flexural wave motions.

The total motion in the finite periodic system can be regarded as the superposition of the motion generated by the given exciting forces when they act on a (doubly) infinite system (the 'infinite system motion') together with the motions reflected back into the system from the finite ends when this infinite system motion impinges on the ends. Denote the magnitude of the infinite system motion by the vector $\{^{+}\Psi_{inf}\}$. Due to this alone, the corresponding displacements and forces at the right hand end of the finite system are (from Eq. s (40a,b))

$$\{^{+}q_R\}_{N_{FR}} = [^{+}\Theta][E^{+\mu}]^{N_{FR}}\{^{+}\Psi_{inf}\} \quad \text{and} \quad \{^{+}F_R\}_{N_{FR}} = -[^{+}\Phi][E^{+\mu}]^{N_{FR}}\{^{+}\Psi_{inf}\}. \qquad (53a,b)$$

The corresponding displacements and forces at the left hand end of the finite system due to $\{^{-}\Psi_{inf}\}$ are

$$\{^{-}q_L\}_{N_{FL}} = [^{-}\Theta][E^{-\mu}]^{N_{FL}}\{^{-}\Psi_{inf}\} \quad \text{and} \quad \{^{-}F_R\}_{N_{FR}} = [^{-}\Phi][E^{-\mu}]^{N_{FL}}\{^{-}\Psi_{inf}\}. \qquad (54a,b)$$

The motion reflected from the left-hand end is that associated with forces acting at the left-hand end of a semi-infinite system as analyzed in Section 4.1 . It will be quantified here by the vector $\{^{+}\Psi_{refl}\}$ of positive-going waves, the corresponding displacements and forces at the left hand end being

$$\{^{+}q_L\}_{LHend} = [\Theta]\{^{+}\Psi_{refl}\} \quad \text{and} \quad \{^{+}F_L\}_{LHend} = [\Phi]\{^{+}\Psi_{refl}\} \qquad (55a,b)$$

At the right hand end of the whole finite system they are

$$\{^{+}q_R\}_{RHend} = [^{+}\Theta][E^{+\mu}]^{N_L}\{^{+}\Psi_{refl}\} \quad \text{and} \quad \{^{+}F_R\}_{RHend} = -[^{+}\Phi][E^{+\mu}]^{N_L}\{^{+}\Psi_{refl}\} \qquad (56a,b)$$

The motion reflected from the right-hand end is that associated with forces acting at the right-hand end of a semi-infinite system as analyzed in Section 4.1. It will be quantified here by the vector $\{^{-}\Psi_{refl}\}$ of negative-going reflected waves. At the right-hand end of the whole system the corresponding displacements and forces are

$$\{^{-}q_R\}_{RHend} = [^{-}\Theta]\{^{-}\Psi_{refl}\} \quad \text{and} \quad \{^{-}F_L\}_{RHend} = -[^{-}\Phi]\{^{-}\Psi_{refl}\} \qquad (57a,b)$$

At the left hand end they are

$$\{^{-}q_R\}_{LHend} = [^{-}\Theta][E^{-\mu}]^{N_L}\{^{-}\Psi_{refl}\} \quad \text{and} \quad \{^{-}F_R\}_{LHend} = [^{-}\Phi][E^{-\mu}]^{N_L}\{^{-}\Psi_{refl}\}. \qquad (58a,b)$$

The total motion due to the two sets of reflected waves and the infinite system motion must satisfy the boundary conditions at the two ends of the finite system. In the special case when both ends of the whole system are free and unconstrained, the total force vectors at each end must be zero so

$$\{^{-}F_L\}_{LHend} + \{^{+}F_L\}_{LHend} + \{^{-}F_{L,\text{inf}}\}_{LHend} = 0 \quad \text{at the left-hand end} \qquad (59a)$$

and

$$\{^{-}F_R\}_{RHend} + \{^{+}F_R\}_{RHend} + \{^{+}F_{\text{inf}}\}_{RHend} = 0 \quad \text{at the right hand end} \qquad (60a)$$

In terms of the Ψ's, Φ's and Θ's these are

$$+[^{-}\Phi][E^{-\mu}]^{N_L}\{^{-}\Psi_{refl}\} + [^{+}\Phi]\{^{+}\Psi_{refl}\} + [^{-}\Phi][E^{-\mu}]^{N_{FL}}\{^{-}\Psi_{\text{inf}}\} = 0 \qquad (61a)$$

and

$$+[^{-}\Phi]\{^{-}\Psi_{refl}\}+[^{+}\Phi][E^{+\mu}]^{N_L}\{^{+}\Psi_{refl}\}+[^{+}\Phi][E^{+\mu}]^{N_{FR}}\{^{+}\Psi_{\inf}\}=0 \tag{61b}$$

Rearrange these into the single matrix equation

$$\begin{bmatrix} [^{-}\Phi][E^{-\mu}]^{N_L} & [^{+}\Phi] \\ [^{-}\Phi] & [^{+}\Phi][E^{+\mu}]^{N_L} \end{bmatrix}\begin{Bmatrix} ^{-}\Psi_{refl} \\ ^{+}\Psi_{refl} \end{Bmatrix}=-\begin{Bmatrix} [^{-}\Phi][E^{-\mu}]^{N_{FL}}\{^{-}\Psi_{\inf}\} \\ [^{+}\Phi][E^{+\mu}]^{N_{FR}}\{^{+}\Psi_{\inf}\} \end{Bmatrix} \tag{62a}$$

so

$$\begin{Bmatrix} ^{-}\Psi_{refl} \\ ^{+}\Psi_{refl} \end{Bmatrix}=-\begin{bmatrix} [^{-}\Phi][E^{-\mu}]^{N_L} & [^{+}\Phi] \\ [^{-}\Phi] & [^{+}\Phi][E^{+\mu}]^{N_L} \end{bmatrix}^{-1}\begin{Bmatrix} [^{-}\Phi][E^{-\mu}]^{N_{FL}}\{^{-}\Psi_{\inf}\} \\ [^{+}\Phi][E^{+\mu}]^{N_{FR}}\{^{+}\Psi_{\inf}\} \end{Bmatrix} \tag{62b}$$

These constitute $2n_C$ equations for the n_C unknown $^{-}\psi$'s and the n_C unknown $^{+}\psi$'s. From the values so obtained one can find the displacement and force at any co-ordinate in the whole system.

5 APPLICATION TO IN-PLANE VIBRATIONS OF THIN FLAT PLATES

5.1 THE MODEL STUDIED

The validity of the method proposed above has been investigated in a study of the simplest of systems - pure in-plane motion of a parallel strip of thin isotropic flat plate. Use has been made of the simplest possible in-plane thin rectangular finite element with four corner nodes, two degrees of freedom per node and all displacements varying linearly over the element. Appendix A gives details of the element stiffness and mass matrices used. The number N_T of elements in a stack was varied from one to six, and the number N_L of stacks per unit length was varied from one to more than 1000. A value of $N_L = 10^{10}$ could have been used with equal facility and with no increase in computing time.

Wave-numbers of the different models have been computed for a wide ND frequency range and are compared with those of the Euler-Bernoulli theory, the Timoshenko beam theory and the simplest longitudinal wave theory. Further comparisons are made with results from the exact elasticity solution for wave propagation in thin plates of finite width. The ND frequency

used is $\omega^2 b^2/(E/\rho)$ where b is the width of the plate and is taken as unity. The wave numbers and decay factors are N_L times the appropriate propagation constant across a single stack of elements.

Some forced vibration results are also presented for single-point excited plates of finite width and infinite length and also of plates (equivalent to thin beams) of finite length. Comparisons are made with results from the Euler-Bernoulli and Timoshenko beam theories. These actually do little more than demonstrate the limited frequency ranges over which these comparator theories are valid.

5.2 Wave numbers calculated by the Finite Element- Periodic Structure theory

Figure 7 shows the wave numbers computed for one element across the width of the plate (N_T = 1) and one per unit length (N_L=1). The decay index and the wave number are plotted (as before) in the positive and negative domains respectively. In this particular case they are actually identical to the propagation constants across the periodic element. Values calculated from the elementary Euler-Bernoulli and Timoshenko beam theories are also shown, together with those from the simplest longitudinal wave theory.

Below the ND frequency of about 1.6 , the FE-PS and E-B wave numbers are in quite close agreement, more so as the frequency decreases, whereas the FE-PS wave numbers and the Timoshenko values are significantly different over this range. On the other hand, the decay indices from FE-PS and Timoshenko are very close. Indeed, the cut-off frequencies at $\Omega = 2$ (which pertain to 'through-the-thickness' shear wave motion) are the same for both theories, provided the Timoshenko shear factor is taken to be 1.0.

The third FE-PS wave number curve (with a cut-off frequency at $\Omega = 3.6$) pertains to symmetric waves which involve mainly tranverse through-the-thickness motion, stretching and compressing the width of the plate. Over the same frequency range the existence of evanescent waves with complex-conjugate wave numbers is suggested. These are 'phantom' waves which belong only to the particular FE model. They do not appear in more realistic models.

It must be emphasized that the Euler-Bernoulli and Timoshenko values which are indicated are not the exact values for in-plane transverse flexural motion of the plate. They are only derived from approximate 'engineering' theories, but the Timoshenko theory is 'exact' within its assumption of a linear x-wise displacement variation across the plate. The FE-PS theory makes the same assumption for its individual elements, so when there is only one element across the depth of the plate ($N_T = 1$), its decay indices approximate closely to those of Timoshenko. As N_T increases, closer agreement is found.

With $N_L = 1$ and $N_T = 1$, the FE-PS wavenumbers cannot extend beyond $\pm\pi$, the value at which all the wave number curves level out. This exposes the deficiency of the FE-PS method for $N_L = 1$ and imposes a severe restriction on the highest frequency at which $N_L = 1$ can yield even reasonably accurate values.

Successive increases in N_L , however, extend this range, as seen in Figures 8 a,b which show values computed for $N_T = 1$, $N_L = 10$ and 1000. Much closer agreement now exists between the FE-PS and Timoshenko values. Indeed, for $N_L = 100$ they are indistinguishable. The decay index curves between $\Omega = 0$ and 2 retain their close agreement whilst the continuous decay index curve descending from 5.6 to 0 has replaced the the curve with the infinite peak for $N_L = 1$. Furthermore, the 'phantom' complex-conjugate wave number curves which appeared for $N_L = 1$ have now disappeared.

The effect of increasing the number of elements in a stack is seen in Figures 9 which have been computed for $N_L = 1024$ and $N_T = 2, 4, 6$. Figures for smaller values values of N_L have not been presented as they serve no further useful purpose.

As N_T increases, the number of possible wave motions at each frequency increases and the wave number curves in particular assume an increasingly confused appearance. At very low frequencies, however, there are never any more than two genuine propagating waves (the simple longitudinal and flexural waves) but as N_T increases there is an increasing number of waves with complex conjugate wave numbers. This leads to the evident increase in number of decay index

curves and the growing apparent confusion in the wave number curves. These curves for complex conjugate waves eventually attach themselves to genuine propagating wave number curves which bulge out negatively to meet them. This is clearly seen on the curves for NT = 6, NE = 1024 at the ND frequency $\Omega = 6.2$. The wave number curve coming down from (approx) $\Omega = 6.4$ to $\Omega = 6.2$ pertains to a genuine propagating wave. At $\Omega = 6.4$ it meets the complex conjugate wave number (coming from the left). As Ω increases from this point, it 'reverses' and increases negatively as a genuine propagating wave. At any frequency between $\Omega = 6.2$ and 6.4 (the left hand part of the bulge) the propagating wave can have two different wave numbers, one of which has phase and group velocities of opposite sign.

It can seen that increasing N_T does not improve the agreement between the FE-PS values and those from the Timoshenko or longitudinal wave theories. This is not unexpected as all of these theories are approximate, and agreement between FE-PS and Timoshenko is only possible when $N_T = 1$.

As N_T increases, the FE-PS theory becomes 'less' approximate and the only satisfactory benchmark values against which to compare its predictions are those from the exact solution to the thin-plate wave equation. The theory for the exact values is presented in Appendix B. The associated computational process is essentially iterative and involves an initial guess at an x-wise wave number, from which an approximate y-wise wave-number is found. These are then refined until they satisfy a transcendental frequency equation representing the edge boundary conditions. The detailed process will not be described here. Suffice it to say that the process is accelerated if the motions which are symmetric or anti-symmetric about the longitudinal plate centre line are studied separately. Accordingly, Figure 10 shows separate comparisons between the FE-PS and exact wave-numbers and decay indices for wave motions which are symmetric or anti-symmetric.

The FE-PS wave numbers are very close to the exact values in the ND frequencies range up to about 4, above which they still follow quite closely the general trend of the exact curves. The low order FE-PS decay indices are also close to the correct values over the same ranges. In particular the lowest order anti-symmetric curve is almost indistinguishable (even on a diagram of much larger scale) from the exact curve, but the decay indices of the higher order evanescent waves

differ considerably from the exact values. The stack of six elements can only predict a finite number of evanescent waves, so even the number of FE-PS decay-index curves differs from those of the exact motion which has an infinite number of such curves. It is not surprising then that the actual values of the higher order FE-PS decay indices differ greatly from those of the exact theory.

5.3 The response to in-plane forces of a finite plate calculated by the FE-PS method

The theory presented in Section 4.5 has next been used to calculate the in-plane response of a finite plate with six stacked elements ($N_T = 6$) and with 1024 elements per unit length ($N_L = 1024$). The overall length of the plate has been taken as ten times its width, so the plate motion is that of a short beam represented by 6 x 1024 x 10 = 61440 elements. The external in-plane harmonic excitation was by two equal vertical forces at one end of the plate acting at the two element nodes closest to the plate centre line (i.e. at the co-ordinates numbered 6 and 8 on Figure 11). These forces constitute an anti-symmetric loading system and can only excite the anti-symmetric modes of the plate (i.e. the flexural modes). Responses were calculated at each of the nodes at the ends of the whole system over the ND frequency range $\Omega = 0$ to 2.0 (i.e. at co-ordinates 6 or 8 on the left hand end element, and at co-ordinates 20 or 22 on the right hand end element.

Figures 12 (a), (b) show the direct and transfer receptances so obtained. The direct receptance in this case is the response at one of the forcing locations to the total force applied at that end. The transfer receptance is the response at the corresponding location at the other end of the system. These receptances are compared on the figures with two curves calculated from the Timoshenko beam theory, one with a Timoshenko shear factor of 1.0 and the other with a shear factor of 0.833[2].

The figures show close agreement between the FE-PS values and those of the Timoshenko theory at low frequencies. The frequencies of the FE-PS resonance peaks over the whole

[2] Ideally, the comparison should be with values obtained from the exact theory of Appendix B, extended to deal with forced harmonic vibration.

frequency range are roughly mid-way between those of the corresponding pair of Timoshenko peaks and, as expected, the Timoshenko peaks for the shear factor of 0.833 are always the lower of each pair. The range of the ND frequency considered in the figures ($\Omega = 0$ to 2.0) is well beyond the range of normal engineering significance as the half wavelength of the motion at $\Omega = 2$ is of the order of the plate width. As the system being considered for Figure 12 is undamped, the height of each peak should be infinite. That they are not is due to the finite frequency resolution used in the calculations..

5.4 The number of waves to be included in the calculation of the total response

An FE array of stacks with N_T elements per stack allows $2(N_T + 1)$ free waves to travel in each direction, leading to $4(N_T+1)$ allowable waves altogether. In the matrix calculations performed for Figure 12 (for $N_T = 6$) all 28 allowable waves were included in the matrix summation for the response. In larger stacks, it may be questioned whether some of these waves could be ignored in order to reduce computing times.

Now the contribution to the response at a given point in the system from any wave or positive-negative pair of waves depends on the frequency, the cross-sectional modes of wave-displacement, the locations and directions of the exciting force and on the response which is required. The determining principle involved in assessing whether a particular wave can be ignored or not is the same as that which leads to the inclusion or omission of a particular mode in a conventional multi-modal forced response calculation for a general dynamic system. The modal characteristics (displacement modse and resonance frequencies) must be known and these, of course, are the eigen-vectors and eigen-values determined in the preliminary eigen-value analysis. The computation time can only be reduced by reducing the degrees of freedom of the system (by reducing the number of elements in the above plate model) which means the use of a less accurate model.

An FE array of stacks with N_T elements per stack allows $2(N_T + 1)$ free waves to travel in each direction, leading to $4(N_T+1)$ allowable waves altogether. In the matrix calculations performed for Figure 10 (for $N_T = 6$) all 28 allowable waves were included in the matrix summation

for the response. In larger stacks, it may be questioned whether some of these waves could be ignored in order to reduce computing times.

Now the contribution to the response at a given point in the system from any wave or positive-negative pair of waves depends on the frequency, the cross-sectional modes of wave-displacement and on the locations and directions of the exciting force and the response which is required. The determining principle involved in assessing whether a particular wave can be ignored or not is the same as that which leads one to include or ignore a particular mode in a conventional forced response calculation for a general dynamic system. The modal characteristics (displacement mode and resonance frequency) must be known and these, of course, are the eigen-vectors and eigen-values determined in the whole eigen-value calculation. The computation time can only be reduced by reducing the degrees of freedom of the system (by reducing the number of elements in the above plate model) which means the use of a less accurate model.

Figures 13 (a), (c) and (e) show the the effect on the response of increasing the number of wave-pairs included in the total, from just one term to the maximum of 14 for $N_T = 6$. Different frequencies have been selected to demonstrate the frequency-dependence of the number of significant waves. The terms have been selected in the order of decreasing decay rate (i.e. term 1 has the greatest decay rate), the decaying waves including those with complex conjugate wave numbers. They are followed in order by the terms for the propagating (non- decaying) waves, in the order of increasing wave number. Shown in Figures 13 (b), (d) and (f) are the moduli of the contributions from each of the 14 wave-pairs. For each figure, the same FE-plate model has been considered as for Figure 12. The ND frequencies (1.75 and 7.65) for Figures 13 (a)-(b) and (e)-(f) are close to resonances whereas for (c)-(d) it is close to an anti-resonance ($\Omega = 1.79$). The relevant excitation forces, their locations and the response locations are indicated in the figure caption.

Close to the anti-resonance at $\Omega = 1.79$ (Figures 13 (c)-(d)) the flexural evanescent wave (term 12) contributes more to the total than the propagating wave (term 14) simply because the positive and negative-going propagating waves do not 'reinforce one another' at anti-resonances. They cancel out, rather than reinforce. Since they contribute so little to the total, the proportion

contributed by other evanescent waves increases. This is clearly observed in Figure 13 (d). Terms 4 and 5, which have significant and identical amplitudes, are evanescent with complex conjugate wave numbers. They are, however, in counterphase so their total contribution vanishes.

Figures 13 (e) and (f) for the resonance at $\Omega = 7.65$ show (as expected) that more propagating waves now participate, as well as their evanescent counterparts. Without investigating in detail the detailed nature of each wave (i.e. its cross-sectional distortion) one cannot state in advance whether or not any one of them is likely to contribute significantly to the total response at a given point. That being so, one cannot state with any certainty how many terms should be included if a reasonable approximation to the response is to be obtained.

Clearly, in the above problem which has symmetry about the longitudinal centre-line, no symmetric wave can be generated when the external forcing is anti-symmetric and no anti-symmetric waves can be generated when the external forcing is symmetric. However, if the boundary conditions are asymmetric at the non-excited end, that boundary can generate symmetric waves as it reflects an incident anti-symmetric wave. This further complicates an assessment of how many wave terms need to be included in a response calculation. The quickest computational procedure is probably to include them all as their eigen-vectors will all be found in any case in the essential eigen-value calculation for the wave numbers.

5. CONCLUSIONS

Periodic structure theory may be conveniently employed in conjunction with the finite element method to reduce computation times for wave numbers and harmonic responses of long uniform beam-type structural components such as rails and uniform stiffeners. Cross sectional distortions are readily taken into account. Very simple elements can be used, their approximate nature being mitigated by making them extremely short in the component lengthwise direction, an indefinitely large number of them being employed in that direction. The whole system is represented as a periodic structure for which the propagation constants (and hence the structural wave numbers) are computed straightforwardly by the methods of periodic structure theory. It has been shown how the corresponding wave motions can be used to calculate forced harmonic responses in infinite and finite systems.

Computation times are independent of the number of elements used in the overall system length, and depend only on the number employed in a single stack around the structural cross section. This alone determines the number of independent free harmonic wave motions predicted by the FE model.

The following conclusions have been drawn from detailed calculations of in-plane wave motion and forced in-plane response of a simple flat plate of finite width:

Very simple flat plate elements can yield adequate accuracy of calculation, provided they are very short in length and very numerous along the system length. Just six elements across the plate width give accurate wave numbers for the propagating waves up to a non-dimensional frequency of 3 or 4, when compared with values calculated from the exact elasticity theory. The evanescent wave numbers is generally of lower accuracy, except for the lowest order wave which corresponds to the Timoshenko evanescent wave. The accuracy increases, as expected, as the number of elements around the cross-section is increased.

The number of waves which make significant contributions to the harmonic in-plane forced response cannot readily be anticipated. It is probably as quick to include them all in the response calculation as to try to determine in advance which of them is likely to make a significant contribution. The high order evanescent waves contributed little to the plate forced response, while the low order evanescent and propagating waves contributed most.

Comparisons made between the calculated flat plate wave numbers and responses and those calculated from the Timoshenko beam theory constitute more of an evaluation of the Timoshenko theory than of the method presented in this paper. Comparisons with the values found from the exact elasticity theory constitute a true evaluation of the present method. The exact method should be extended to predict the exact forced responses as the basis for a complete evaluation.

REFERENCES

1. D.J.MEAD A general theory of harmonic wave propagation in linear periodic systems with multiple coupling. *Journal of Sound and Vibration* (1973) **27**, 235-260.

2. B. AALAMI Waves in prismatic guides of arbitrary cross section. *Journal of Applied Mechanics* (1973) **40**, 1067-1072.

3. L. BRILLOUIN Wave propagation in periodic structures. Dover Publications, Inc. New York, 1953

4. D.J.MEAD Wave propagation and natural modes in periodic systems: II. Multi-coupled systems, with and without damping. *Journal of Sound and Vibration* (1975) **40**, 19-39.

5. D.J.MEAD Free wave propagation in periodically supported, infinite beams. *Journal of Sound and Vibration* (1970) **11**, 181-197

6. D.J.MEAD, D-C. ZHU and N.S. BARDELL Free vibration of an orthogonally stiffened flat plate. *Journal of Sound and Vibration* (1988) **127**, 19-48.

7. N.S.BARDELL and D.J.MEAD Free vibration of an orthogonally stiffenened cylindrical shell, Part I: Discrete line simple supports. *Journal of Sound and Vibration* (1989) **134**, 29-54.

8. R.M.ORRIS and M.PETYT A finite element study of harmonic wave propagation in periodic structures. *Journal of Sound and Vibration* (1974) **33**, 223-236.

9. A.L.ABRAHAMSON Flexural wave mechanics - an analytical approach to the vibration of periodic structures forced by convected pressure fields. *Journal of Sound and Vibration* (1973) **28**, 247-258.

10. D.J.THOMPSON Wheel-rail noise generation, Part III: rail vibration. *Journal of Sound and Vibration* (1993) **161**, 423-446.

11. L.GAVRIC Computation of propagative waves in free rail using a finite element technique. *Journal of Sound and Vibration* (1995) **185**, 531-543

12. S. WIDEHAMMER 2003 *Journal of Sound and Vibration* **259**, 893-915 Estimation of field quantities and energy flux associated with elastic waves in a bar.

13. S. FINNVEDEN Evalution of modal density and group velocity by a finite element method. *Journal of Sound and Vibration* (2004) **273**, 51-75.

14. C-M NILSSON Waveguide elements applied to a car tyre. Doctoral Thesis, Royal Institute of Technology, Stockholm, Sweden (2004).

15. B R MACE, D DUHAMEL, N J BRENNAN, L HINKE Finite element prediction of wave motion in structural waveguides. *Journal of the Acoustical Society of America* (2005) **117**, 2835- 2843.

APPENDIX A

THE STIFFNESS AND MASS MATRICES OF THE SIMPLE RECTANGULAR THIN PLATE FINITE ELEMENT

Figure A1 shows the rectangular element and the numbering system used for the eight displacement coordinates assigned to the four corners of the element. The whole displacement vector is to be arranged in the order $\{u_1, v_1, u_2, v_2, u_3, v_3, u_4, v_4\}^T$

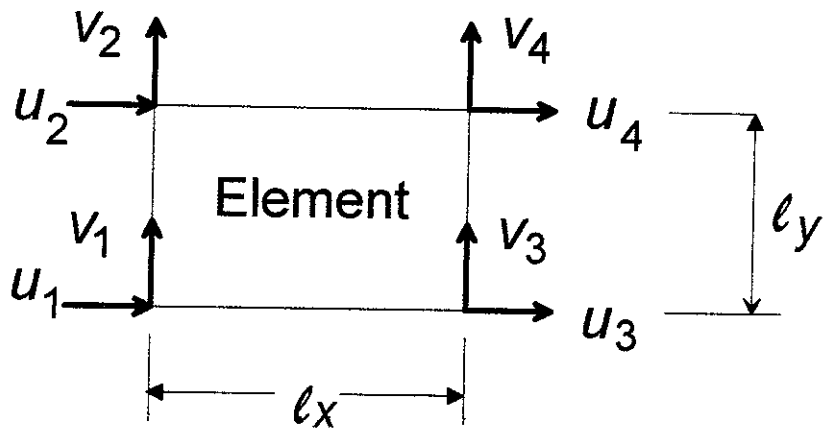

Figure A1 Diagram showing the displacement coordinates and numbering system for the rectangular thin-plate finite element.

The element is assumed to be thin enough for the plane-stress stress-strain relationships to apply. By imposing linear variations of all displacements across the element and by using symbolic computing to manipulate the appropriate matrix equations, the following stiffness and mass matrices were obtained.

$$K_e = \left[K1(\nu)\frac{l_y}{l_x} + K2(\nu)\frac{l_x}{l_y} + K3(\nu)\right]\frac{Eh}{3(1-\nu^2)} \qquad \text{(A1)}$$

where $K1(\nu)$, $K2(\nu)$ and $K3(\nu)$ are non-dimensional matrices defined below and are functions only of the plate Poisson's ratio ν. E is the plate Young's modulus; h is its thickness.

$$K1 = \begin{bmatrix} 1 & 0 & 1/2 & 0 & -1 & 0 & -1/2 & 0 \\ 0 & n_1 & 0 & n_1/2 & 0 & -n_1 & 0 & -n_1/2 \\ 1/2 & 0 & 1 & 0 & -1/2 & 0 & -1 & 0 \\ 0 & n_1/2 & 0 & n_1 & 0 & -n_1/2 & 0 & -n_1 \\ -1 & 0 & -1/2 & 0 & 1 & 0 & 1/2 & 0 \\ 0 & -n_1 & 0 & -n_1/2 & 0 & n_1 & 0 & n_1/2 \\ -1/2 & 0 & -1 & 0 & 1/2 & 0 & 1 & 0 \\ 0 & -n_1/2 & 0 & -n1 & 0 & n_1/2 & 0 & n_1 \end{bmatrix} \quad \text{(A2a)}$$

$$K2 = \begin{bmatrix} n_1 & 0 & -n_1 & 0 & n_1/2 & 0 & -n_1/2 & 0 \\ 0 & 1 & 0 & -1 & 0 & 0.5 & 0 & -0.5 \\ -n_1 & 0 & n_1 & 0 & -n_1/2 & 0 & n_1/2 & 0 \\ 0 & -1 & 0 & 1 & 0 & -0.5 & 0 & 0.5 \\ n_1/2 & 0 & -n_1/2 & 0 & n_1 & 0 & -n_1 & 0 \\ 0 & 0.5 & 0 & -0.5 & 0 & 1 & 0 & -1 \\ -n_1/2 & 0 & n_1/2 & 0 & -n_1 & 0 & n_1 & 0 \\ 0 & -0.5 & 0 & 0.5 & 0 & -1 & 0 & 1 \end{bmatrix} \quad \text{(A2b)}$$

$$K3 = \begin{bmatrix} 0 & n_2 & 0 & n_3 & 0 & -n_3 & 0 & -n_2 \\ n_2 & 0 & -n_3 & 0 & n_3 & 0 & -n_2 & 0 \\ 0 & -n_3 & 0 & -n_2 & 0 & n_2 & 0 & n_3 \\ n_3 & 0 & -n_2 & 0 & n_2 & 0 & -n_3 & 0 \\ 0 & n_3 & 0 & n_2 & 0 & -n_2 & 0 & -n_3 \\ -n_3 & 0 & n_2 & 0 & -n_2 & 0 & n_3 & 0 \\ 0 & -n_2 & 0 & -n_3 & 0 & n_3 & 0 & n_2 \\ -n_2 & 0 & n_3 & 0 & -n_3 & 0 & n_2 & 0 \end{bmatrix} \quad \text{(A2c)}$$

In these $n_1 = \frac{1-\nu}{2}$ $n_2 = \frac{3}{8}(1+\nu)$ $n_3 = \frac{3}{8}(1-3\nu)$

The mass matrix for the element is found in a similar way to be:

$$M = \begin{bmatrix} 1 & 0 & 1/2 & 0 & 1/2 & 0 & 1/4 & 0 \\ 0 & 1 & 0 & 1/2 & 0 & 1/2 & 0 & 1/4 \\ 1/2 & 0 & 1 & 0 & 1/4 & 0 & 1/2 & 0 \\ 0 & 1/2 & 0 & 1 & 0 & 1/4 & 0 & 1/2 \\ 1/2 & 0 & 1/4 & 0 & 1 & 0 & 1/2 & 0 \\ 0 & 1/2 & 0 & 1/4 & 0 & 1 & 0 & 1/2 \\ 1/4 & 0 & 1/2 & 0 & 1/2 & 0 & 1 & 0 \\ 0 & 1/4 & 0 & 1/2 & 0 & 1/2 & 0 & 1 \end{bmatrix} \frac{\rho h l_x l_y}{9} \tag{A3}$$

The global matrices formed from these for the single stack of N_T elements lead to the following global equations relating the stack displacements and forces

$$\left[[Kg]\frac{Eh}{3(1-\nu^2)} - \omega^2[M_g]\frac{\rho h l_x l_y}{9}\right]\begin{Bmatrix}(u,v)_L \\ (u,v)_R\end{Bmatrix} = \begin{Bmatrix}F_L \\ F_R\end{Bmatrix}$$

$$\text{i.e} \quad \left[[Kg](1-\nu^2)^{-1} - [M_g]\tfrac{1}{3}\left(\frac{\omega^2\rho l_x l_y}{E}\right)\right]\begin{Bmatrix}(u,v)_L \\ (u,v)_R\end{Bmatrix} = \begin{Bmatrix}F_L \\ F_R\end{Bmatrix}\frac{3}{Eh}$$

For a plate of width b, $l_y = b/N_T$. The unit plate length is also taken as b, so $l_x = 1/N_E$. Hence

$$\left(\frac{\omega^2\rho l_x l_y}{E}\right) = \left(\frac{\omega^2\rho b^2}{E}\right)\frac{1}{N_T N_E} = \Omega^2\frac{1}{N_T N_E}$$

With b set equal to unity, Ω becomes the ND frequency used in this paper and the above matrix equation can take the form

$$[D(\Omega, N_T, N_L, \nu]\begin{Bmatrix}(u,v)_L \\ (u,v)_R\end{Bmatrix} = \begin{Bmatrix}F_L \\ F_R\end{Bmatrix}\frac{3}{Eh}$$

in which $[D(\Omega, N_T, N_E, \nu] = \left[[Kg](1-\nu^2)^{-1} - \Omega^2[M_g]\frac{1}{3N_T N_E}\right]$ is the non-dimensional dynamic stiffness matrix for the stack of NT elements and has been used for all the plate calculations of this paper.

APPENDIX B

EQUATIONS FOR THE EXACT WAVE NUMBERS OF IN-PLANE WAVE MOTION IN A THIN UNIFORM ISOTROPIC PLATE OF FINITE WIDTH

In terms of the displacements $u(x,y)$, $v(x,y)$ in the x- and y-directions, the plane-stress equations of harmonic motion of a thin plate of unit thickness are

$$\frac{E}{(1-\nu^2)}\left\{\frac{\partial^2 u}{\partial x^2}+\left(\frac{1-\nu}{2}\right)\frac{\partial^2 u}{\partial y^2}\right\}+\omega^2\rho u+\frac{E}{(1-\nu^2)}\left\{\left(\frac{1+\nu}{2}\right)\frac{\partial^2 v}{\partial x\partial y}\right\}=0 \tag{B1}$$

and

$$\frac{E}{(1-\nu^2)}\left\{\left(\frac{1+\nu}{2}\right)\frac{\partial^2 u}{\partial x\partial y}\right\}+\omega^2\rho v+\frac{E}{(1-\nu^2)}\left\{\frac{\partial^2 v}{\partial y^2}+\left(\frac{1-\nu}{2}\right)\frac{\partial^2 v}{\partial x\partial y}\right\}=0 \tag{B2}$$

Admissible plane wave motions have the general form

$$u(x,y)=U\exp(\lambda_x x/b)\exp(\lambda_y y/b),\qquad v(x,y)=V\exp(\lambda_x x/b)\exp(\lambda_y y/b) \tag{B3}$$

Substituting these into equations B1, B2 yields the matrix equation

$$\begin{bmatrix} \lambda_x^2+\frac{(1-\nu)}{2}\lambda_y^2+\Omega^2(1-\nu^2) & \frac{1+\nu}{2}\lambda_x\lambda_y \\ \frac{1+\nu}{2}\lambda_x\lambda_y & \lambda_y^2+\frac{(1-\nu)}{2}\lambda_x^2+\Omega^2(1-\nu^2) \end{bmatrix}\begin{Bmatrix} U \\ V \end{Bmatrix}=0 \tag{B4}$$

in which the non-dimensional frequency $\Omega=\sqrt{\dfrac{\omega^2\rho b^2}{E}}$ (B5)

b is the plate width.

The determinant of the 2 x 2 matrix in Eqn (B4) must vanish. Expand it, equate it to zero and solve the bi-quadratic equation for λ_y in terms of λ_x and Ω to yield the following four solutions:

$$\lambda 1_y = \pm\sqrt{-\lambda_x^2 - (1-\nu^2)\Omega^2}\,, \qquad \lambda 2_y = \pm\sqrt{-\lambda_x^2 - 2(1+\nu)\Omega^2}. \tag{B6a,b}$$

Corresponding to these are the V/U relationships

$$(V/U)_1 = -\frac{\lambda_x^2+\lambda 1_y^2(1-\nu)/2+\Omega^2(1-\nu^2)}{\lambda_x \lambda 1_y(1+\nu)/2} \quad \text{and} \quad (V/U)_2 = -\frac{\lambda_x^2+\lambda 2_y^2(1-\nu)/2+\Omega^2(1-\nu^2)}{\lambda_x \lambda 2_y(1+\nu)/2}$$

which simplify to

$$(V/U)_1 = i\sqrt{1+(1-\nu^2)\frac{\Omega^2}{\lambda_x^2}} \quad \text{and} \quad (V/U)_2 = i/\sqrt{1+2(1+\nu)\frac{\Omega^2}{\lambda_x^2}} \tag{B7a,b}$$

Free wave motion along the infinite plate must satisfy the boundary conditions along the top and bottom edges at y = $\pm b/2$. If these edges are stress-free, then

$$\sigma_y = \frac{E}{(1-\nu^2)}\left(\nu\frac{\partial u}{\partial x} + \frac{\partial v}{\partial y}\right) = 0 \qquad \tau_{xy} = \frac{E}{2(1+\nu)}\left(\frac{\partial v}{\partial x} + \frac{\partial u}{\partial y}\right) = 0. \text{ at } y = \pm b/2$$

For computational purposes it is convenient to consider wave motions which are either symmetric or anti-symmetric about the plate longitudinal centre-line ($y = 0$). Satisfaction of the boundary conditions at $y = +b/2$ then automatically satisfies the conditions at $y = -b/2$ so only two boundary conditions need to be considered explicitly. The y-wise dependence of symmetric and anti-symmetric motions can therefore be represented respectively by

$$U(y) = A_1 \cosh \lambda 1_y y + A_2 \cosh \lambda 2_y y \qquad V(y) = B_1 \sinh \lambda 1_y y + B_2 \sinh \lambda 2_y y \qquad \text{(symmetric)}$$

$$U(y) = A_1 \sinh \lambda 1_y y + A_2 \sinh \lambda 2_y y \qquad V(y) = B_1 \cosh \lambda 1_y y + B_2 \cosh \lambda 2_y y \qquad \text{(anti-symmetric)}$$

The corresponding pairs of boundary conditions are then represented by the matrix equations:

$$\begin{bmatrix} (\lambda_x(V/U)_1 + \lambda 1_y)\sinh \lambda 1_y b/2 & (\lambda_x(V/U)_2 + \lambda 2_y)\sinh \lambda 2_y b/2 \\ (\nu\lambda_x + (V/U)_1 \lambda 1_y)\cosh \lambda 1_y b/2 & (\nu\lambda_x + (V/U)_2 \lambda 2_y)\cosh \lambda 2_y b/2 \end{bmatrix} \begin{Bmatrix} A_1 \\ A_2 \end{Bmatrix} = 0 \quad \text{(symm)} \qquad \text{(B8a)}$$

$$\begin{bmatrix} (\lambda_x(V/U)_1 + \lambda 1_y)\cosh \lambda 1_y b/2 & (\lambda_x(V/U)_2 + \lambda 2_y)\cosh \lambda 2_y b/2 \\ (\nu\lambda_x + (V/U)_1 \lambda 1_y)\sinh \lambda 1_y b/2 & (\nu\lambda_x + (V/U)_2 \lambda 2_y)\sinh \lambda 2_y b/2 \end{bmatrix} \begin{Bmatrix} A_1 \\ A_2 \end{Bmatrix} = 0 \quad \text{(anti-symm)} \quad \text{(B8b)}$$

Equating the determinants of the two matrices to zero and expanding them leads to transcendental equations from which the satisfying pairs of λ_x's and λ_y's can be found for any given frequency. These λ's may be real, imaginary or complex and occur in positive/negative and conjugate pairs.

Figures

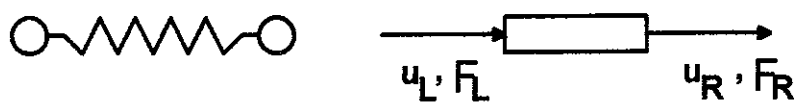

Figure 1 The mass-spring model of the bar element, and the notation used for its displacement co-ordinates and forces .

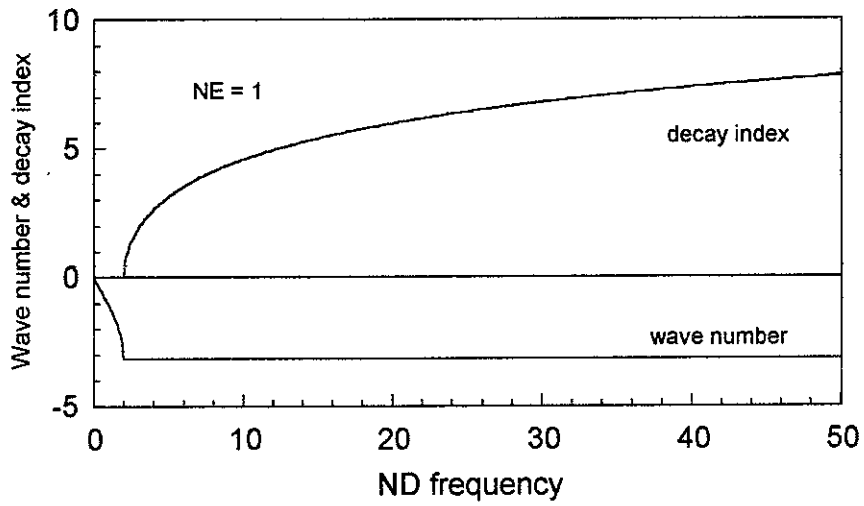

Figure 2 Wave numbers of a uniform bar as calculated by the FE-PS method for $N_E = 1$

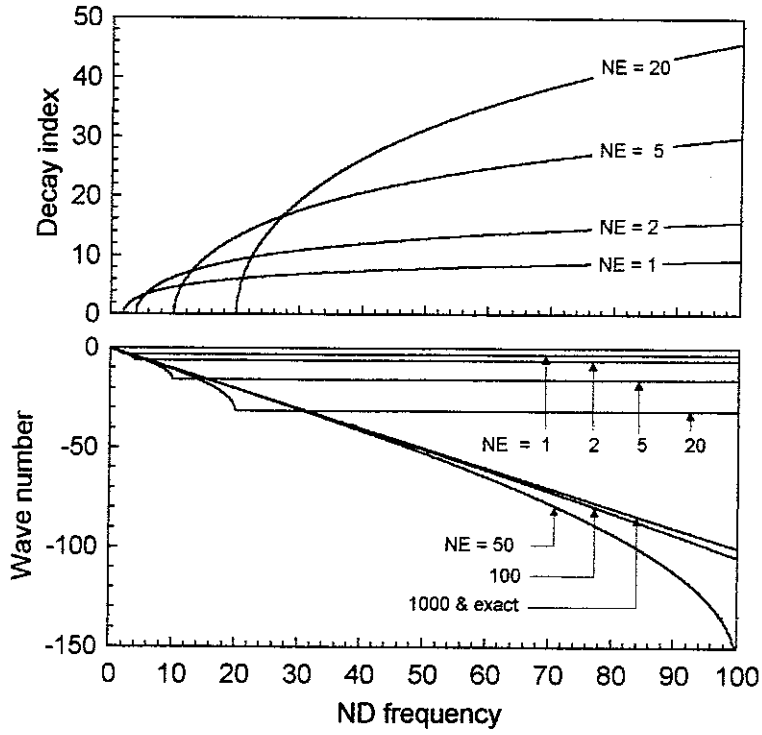

Figure 3 Wave numbers of a uniform bar as calculated by the FE-PS method; N_E = 1 to 1000

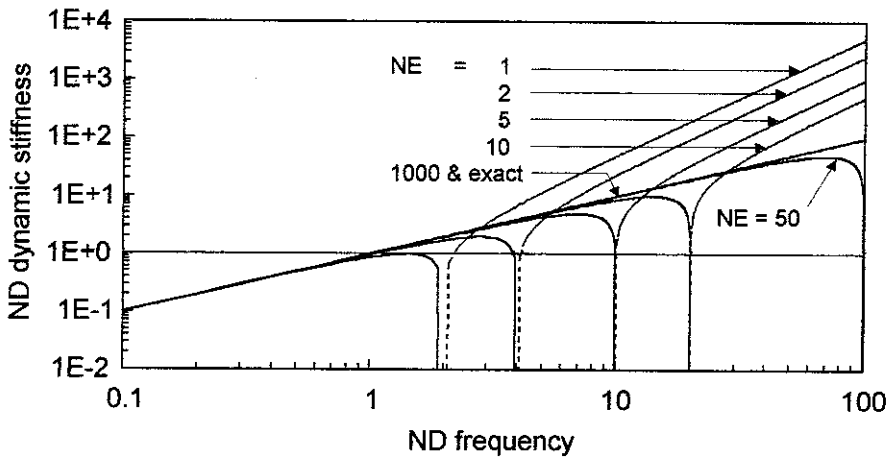

Figure 4 The dynamic stiffness at the free end of a semi-infinite bar calculated by the FE-PS method. ——— , imaginary parts; - - - - - - , real parts.

Figure 4 Receptances of a finite bar as calculated by the FE-PS method for different values of NE

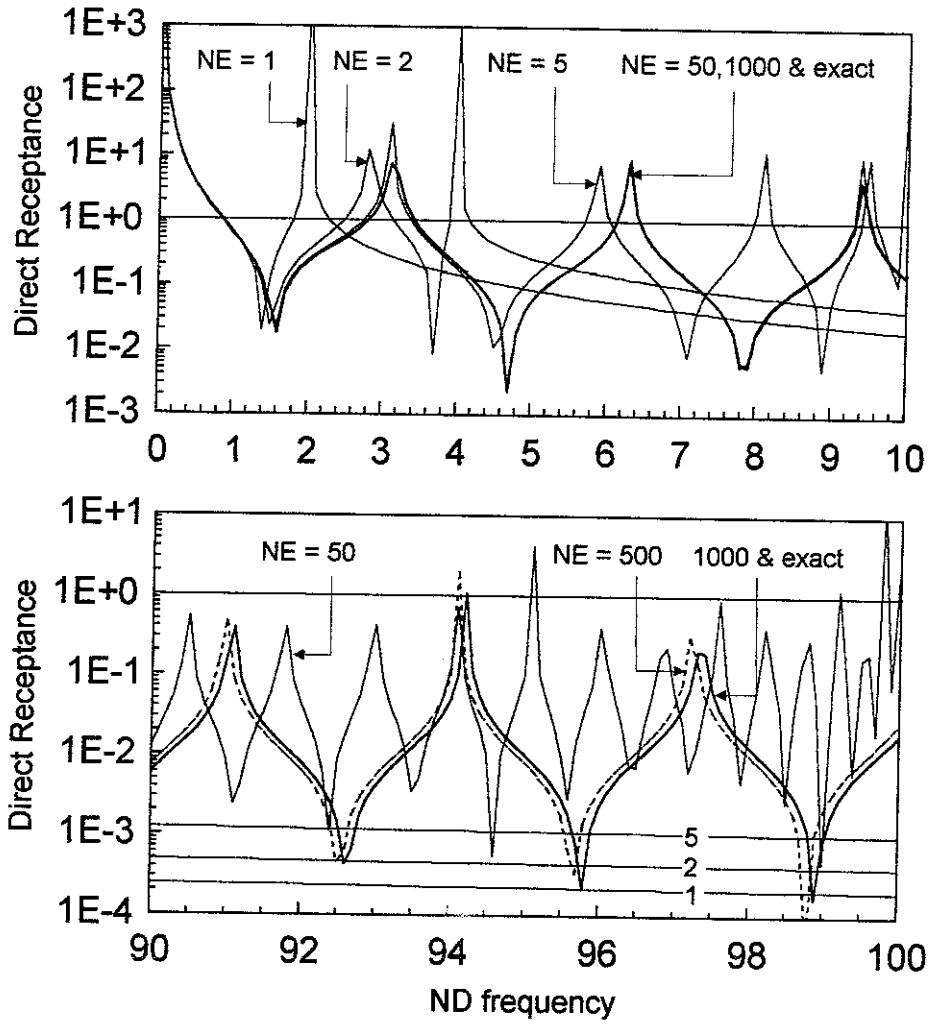

Figure 5 Direct receptance at the loaded end of an axially-excited uniform bar as calculated by the FE-PS method.

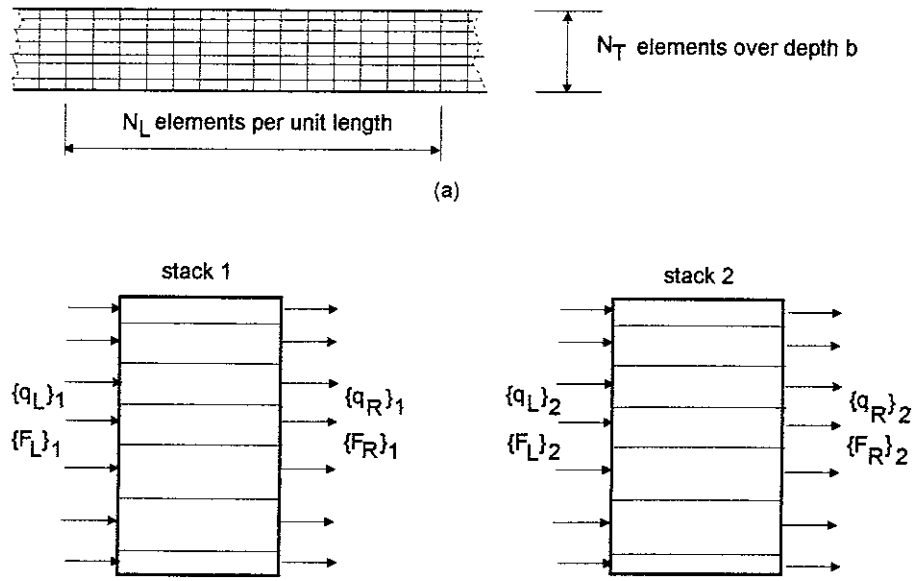

Figure 6 (a) The whole array of finite elements (b) the forces and coordinate systems for two adjacent stacks of elements

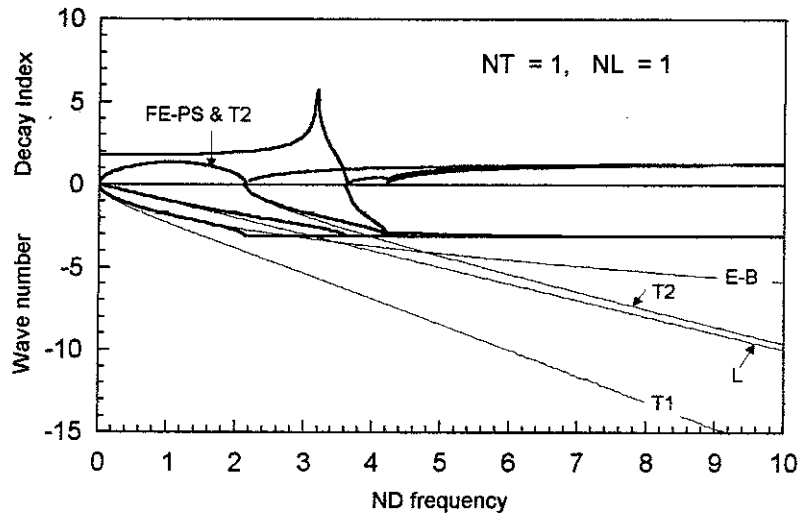

Figure 7 Decay index and wave number as calculated by the FE-PS method for $N_T = 1$, $N_L = 1$. E-B, values from the Euler-Bernoulli beam theory; L, values from the simplest longitudinal wave theory; T1 and T2, values from the Timoshenko beam theory.

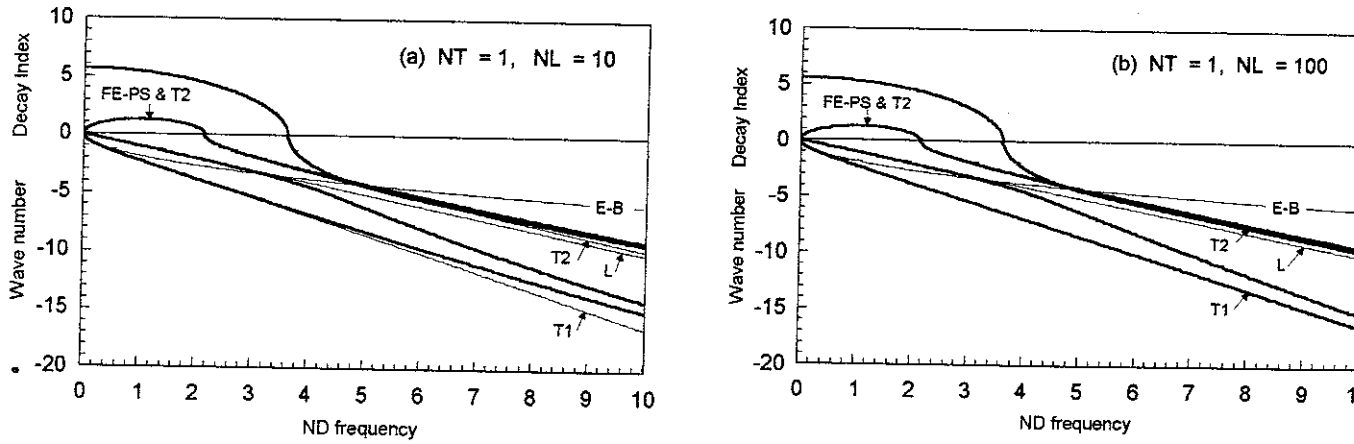

Figure 8 Decay indices and wave numbers as calculated by the FE-PS method for (a) $N_T = 1$, $N_L = 10$ (b) $N_T = 1$, $N_L = 100$. E-B, values from the Euler-Bernoulli beam theory; L, values from the simplest longitudinal wave theory; T1 and T2, values from the Timoshenko beam theory

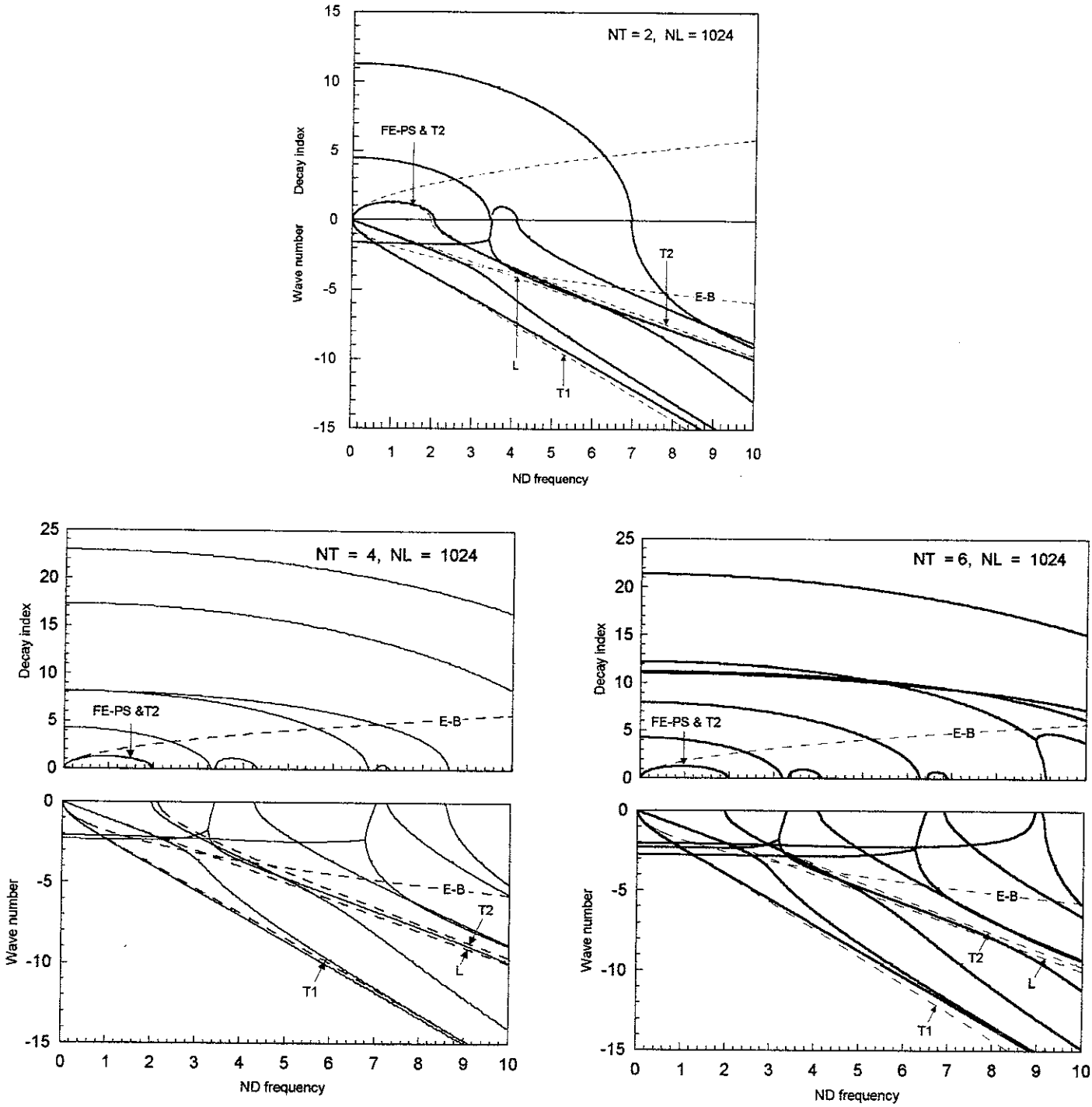

Figure 9 Decay indices and wave numbers calculated by the FE-PS method for $N_T = 2$, 4 and 6; $N_L = 1024$. Timoshenko (T1 & T2, unit shear factor), Euler-Bernoulli (E-B) and simple longitudinal values (L) are also indicated.

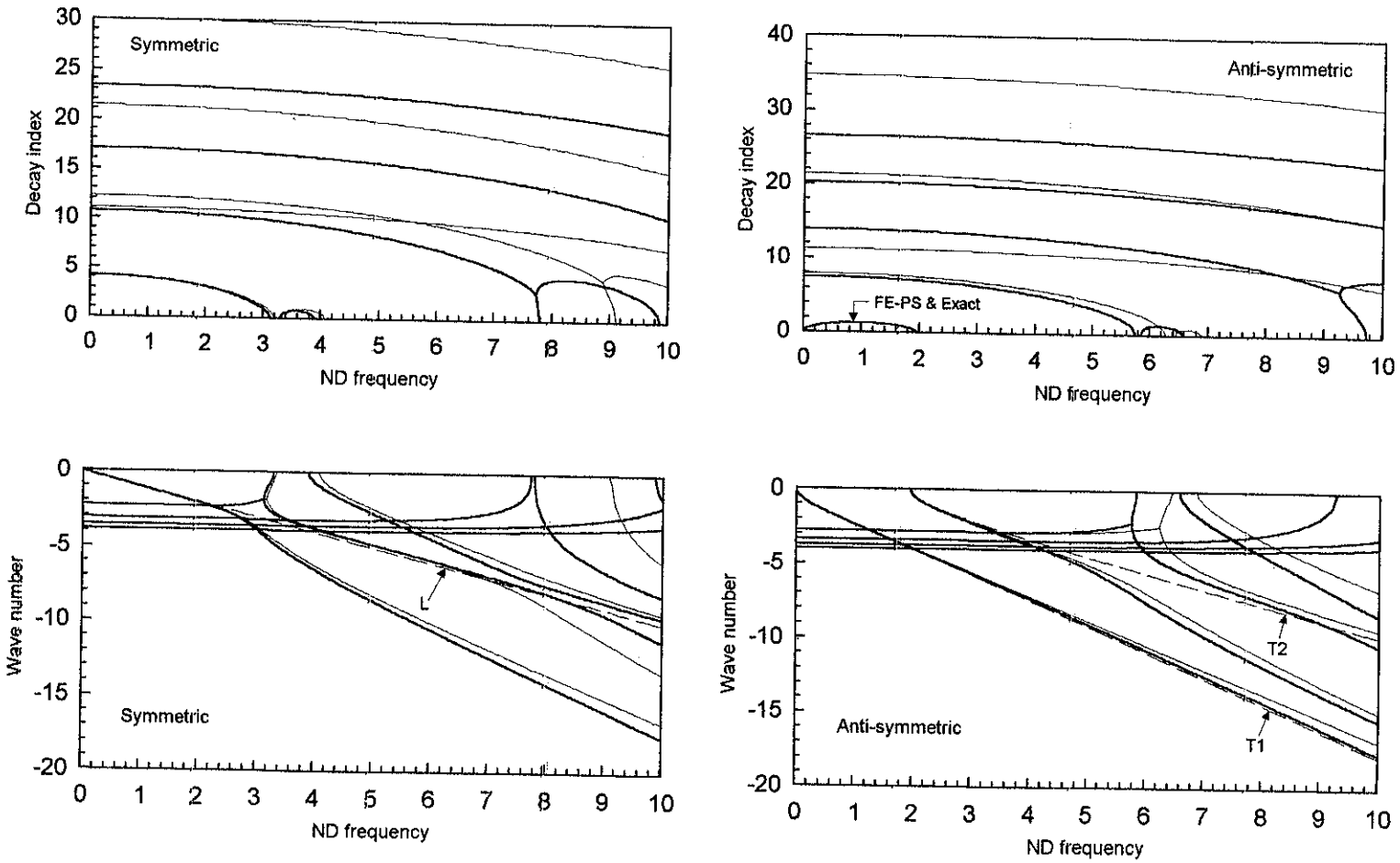

Figure 10 Decay indices and wave numbers calculated by the FE-PS method for $N_T = 6$, $N_L = 1024$ compared with exact values. Thin lines, FE-PS values; thick lines, exact values. T1 & T2, Timoshenko values (unit shear factor). L, values from the elementary longitudinal wave theory

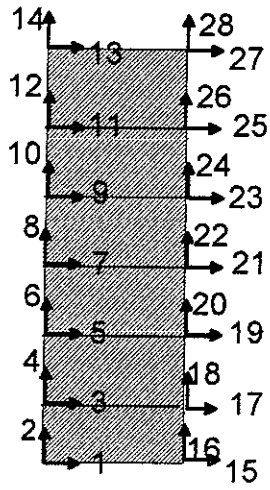

Figure 11 Coordinate numbering system for the stack of six finite elements representing part of the flat plate

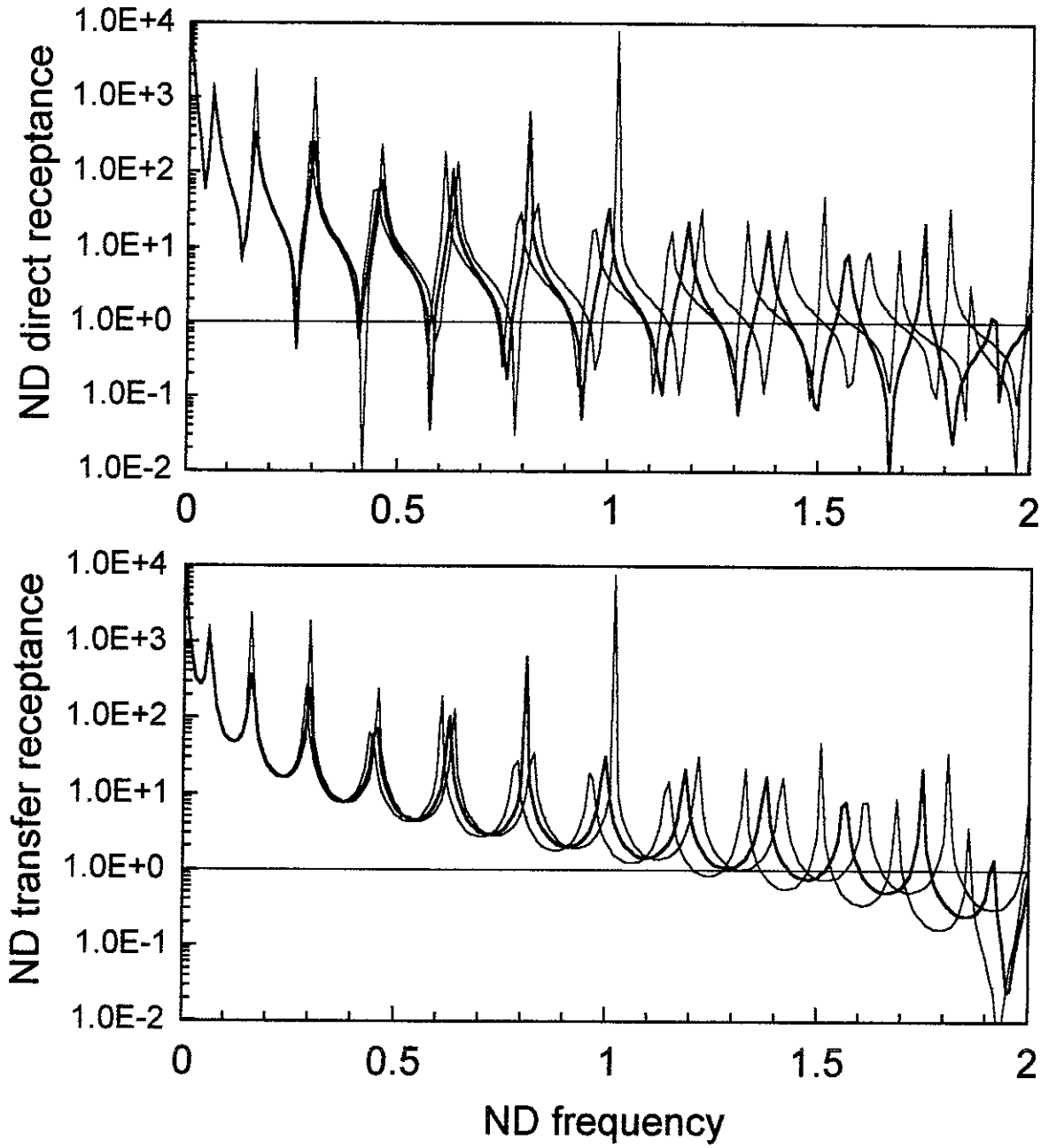

Figure 12 Receptances of a thin finite plate to vertical forces at one end. Plate length = 10 x depth. ----------, FE-PS results; - - - - -, Timoshenko theory, shear factor = 1.0; ------ ------ ; Timoshenko theory, shear factor = 0.833. Two equal external forces of 0.5 exist at co-ordinates 6 & 8. The receptances relate to coordinate 8 at the end of the extreme LH element and to coordinate 22 at the end of the extreme RH element. $N_T = 6$, $N_L = 1024$, Length of plate = 10 x width

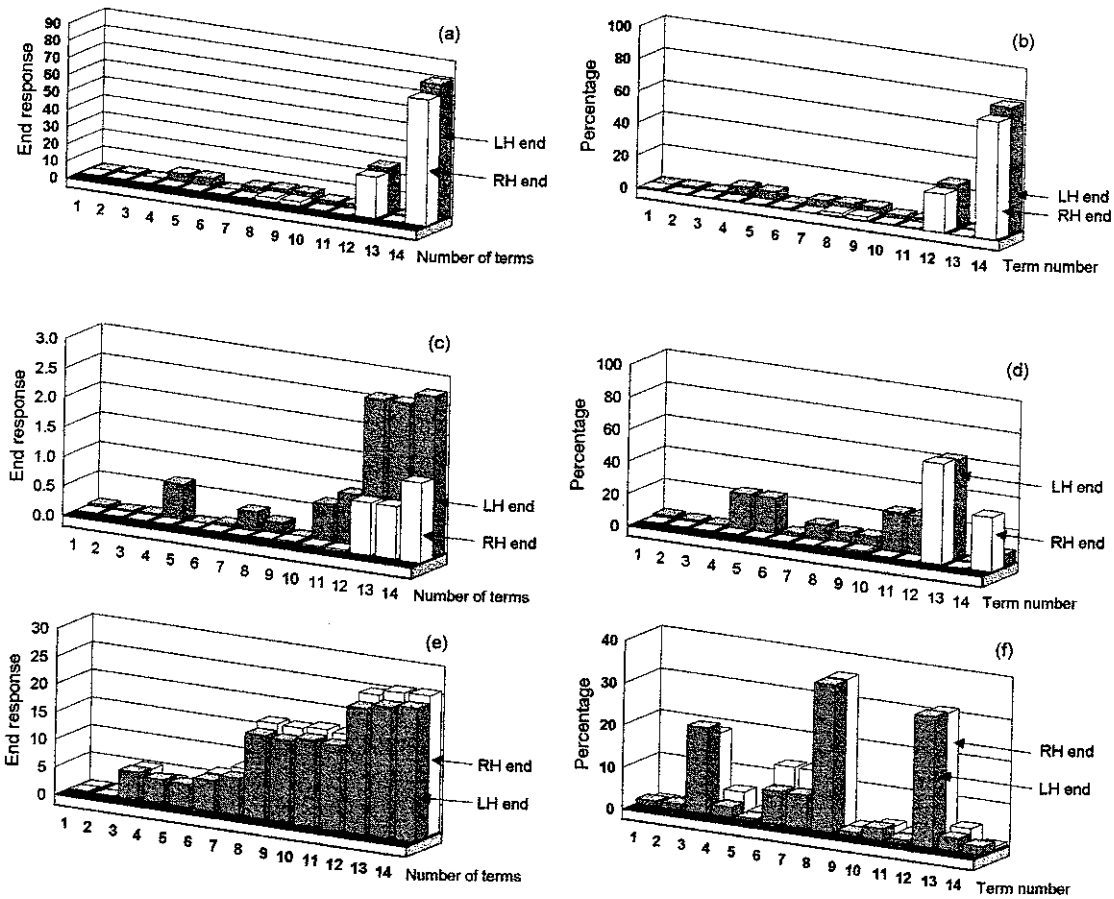

Figure 13 (a), (c) & (e): Diagrams showing the effect of increasing the number of terms in the series expression for the plate receptances at different frequencies. (b), (d) & (f): the contributions from each term. (a) & (b) ND frequency = 1.75, equal forces of 0.5 at co-ordinates 6 & 8, response location at coordinate 6; (c) & (d) ND frequency = 1.79, unit force at coordinate 10, response location at coordinate 1 (e) & (f): ND frequency = 7.65, unit force at coordinate 10, response location at coordinate 2. In each case, NT = 6, NE = 1024, L = 10.

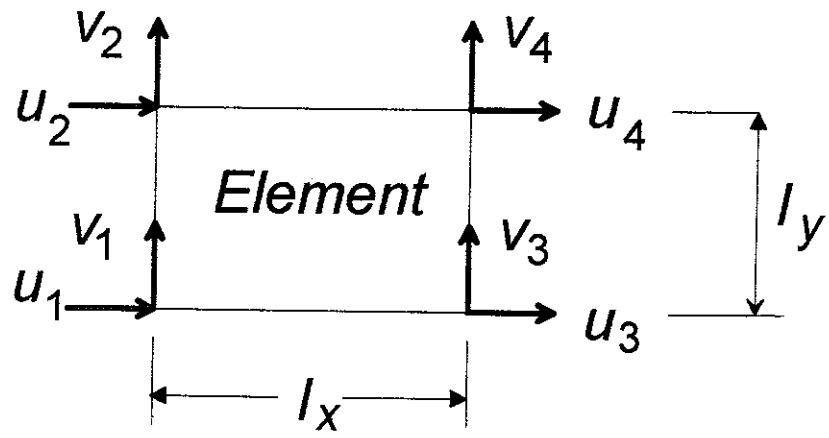

Figure A1 Diagram showing the displacement coordinates and numbering system for the thin-plate rectangular finite element.